# Synthesis and Characterization of Novel Acyl-Glycine Inhibitors of GlyT2

**Shannon N. Mostyn[1], Jane E. Carland[1,] Susan Shimmon[2], Renae M. Ryan[1], Tristan Rawling[2] and Robert J. Vandenberg[1,3]**

1. **Discipline of Pharmacology, School of Medical Sciences, University of Sydney, Sydney, NSW, 2006, Australia**
2. **School of Mathematical and Physical Sciences, Faculty of Science, The University of Technology Sydney, Sydney, NSW, 2007, Australia**
3. **Corresponding author email: robert.vandenberg@sydney.edu.au**

**Key words: Glycine Transport Inhibition, acyl-glycine, analgesia, GlyT2**

## ABSTRACT

It has been demonstrated previously that the endogenous compound N-arachidonyl-glycine inhibits the glycine transporter GlyT2, stimulates glycinergic neurotransmission, and provides analgesia in animal models of neuropathic and inflammatory pain. However, it is a relatively weak inhibitor with an $IC_{50}$ of 9 µM and is subject to oxidation via cyclooxygenase limiting its therapeutic value. In this paper we describe the synthesis and testing of a novel series of mono-unsaturated C18 and C16 acyl-glycine molecules as inhibitors of the glycine transporter GlyT2. We demonstrate that they are up to 28 fold more potent that N-arachidonyl-glycine with no activity at the closely related GlyT1 transporter at concentrations up to 30 µM. This novel class of compounds show considerable promise as a first generation of GlyT2 transport inhibitors.


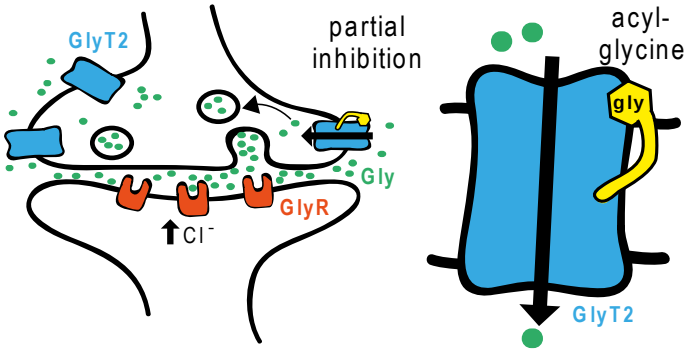

## INTRODUCTION

Lipids are increasingly acknowledged for having important interactions with membrane proteins, as both the environment in which membrane proteins operate[1], and as ligands which can impart changes in activity[2-5]. Arachidonylethanolamide (anandamide) is one of the most recognised lipid ligands and is proposed to exhibit its agonist effects by accessing the binding site of cannabinoid (CB) receptors via the cell membrane[6, 7]. N-arachidonyl glycine (NAGly) is a carboxylic acid derivative of anandamide (Figure 1) which is endogenously produced through two distinct enzymatic pathways[8] in the central nervous system. NAGly is found in highest concentrations within the spinal cord and may play an important role in modulating pain[9]. Intrathecal injection of NAGly reduces mechanical allodynia and thermal hyperalgesia in rat models of both neuropathic and inflammatory chronic pain[10, 11]. Furthermore, co-application of NAGly with $CB_1$ or $CB_2$ receptor antagonists does not disrupt the analgesic effects of NAGly which is consistent with early binding studies of anandamide derivatives that show NAGly has negligible activity at cannabinoid receptors[12], which raises the question as to how NAGly mediates its analgesic activity. One possible mechanism of action is modulation of glycinergic neurotransmission. NAGly prolongs the time course of glycine in glycinergic synapses of lamina II of the superficial dorsal horn[13], an area responsible for integrating ascending pain information. It has been shown that NAGly inhibits the glycine transporter GlyT2, but has no effect on the closely related glycine transporter GlyT1[14], which suggests that NAGly may exert analgesia by increasing inhibitory tone at glycinergic neurons.

Inhibitory glycinergic neurons play an important role within the spinal cord where they are expressed predominantly in lamina III and V of the dorsal horn[15] and project to the brain to modulate signalling. Recently, in a rat nerve ligation model of neuropathic

pain, it has been shown that excitatory radial neurons in lamina II have impaired glycinergic inputs[16] which is likely to cause incorrect processing of sensory information in the dorsal horn and can lead to a neuropathic pain phenotype. Increasing glycinergic signalling, via inhibition of glycine transport, could therefore be an effective strategy to repair this dysfunction.

Glycinergic neurotransmission is tightly regulated through $Na^+/Cl^-$ dependent glycine transporters[17] which govern the synaptic concentrations of glycine and are responsible for terminating neurotransmission by rapidly transporting glycine back into cells. The two subtypes of glycine transporters, GlyT1 and GlyT2, are differentially expressed, with GlyT1 being ubiquitously expressed in both inhibitory and excitatory synapses, and GlyT2 almost exclusively occupying the membranes of presynaptic inhibitory glycinergic neurons[18]. Selective inhibition of GlyT2 is therefore uniquely located to modulate inhibitory tone and signalling in the ascending pain pathway.

GlyT2 is an essential protein; knock out of the GlyT2 gene in mice produces severe neuromotor symptoms and is lethal two weeks postnatal[19]. The consequences of this deletion are presynaptic in origin, which suggests GlyT2 plays a crucial role in maintaining the pool of glycine to be loaded into vesicles for exocytotic release. ORG-25543 is a full and irreversible GlyT2 inhibitor which also exhibits an excitotoxic phenotype that may mimic the GlyT2 knock out effects, and is likely a result of disrupted vesicle filling and therefore a decrease in glycine in the synapse in the long-term[20, 21]. Conversely, partial reduction in GlyT2 expression using siRNA does not produce the hyperekplexia like symptoms generated by GlyT2 knock outs or full inhibitors. Additionally, targeted partial knock down of GlyT2 has been shown to be analgesic in neuropathic pain models in mice,[22] validating the value of partial inhibitors of GlyT2. Partial non-competitive glycine transport inhibitors are likely to slow the

clearance rate of glycine from the synapse, but not block it completely and thereby still allow accumulation of presynaptic glycine that is sufficient for recycling. NAGly is also a partial non-competitive inhibitor of GlyT2, and does not generate any overt motor side effects[10, 11], suggesting that compounds like NAGly have potential for the treatment of pain with minimal side effects.

Although exogenous NAGly has been shown to be efficacious for the treatment of pain, its utility is limited by its rapid metabolism[23], low potency at GlyT2 ($IC_{50}$ 9 µM)[14] and role as a non-specific signalling molecule[9, 23]. COX-2 is present in high concentrations in tissues rich in NAGly and inactivates the molecule through a cyclisation reaction at its ω6 polyunsaturated arachidonyl tail[23]. One strategy to circumvent, or slow the metabolism of a GlyT2 lipid inhibitor is to alter the lipid tail of the compound. Previously our group has reported the activity of N-oleoyl glycine (NOGly) as an inhibitor of GlyT2[24]. NOGly similarly contains a glycine head group and has instead, an ω9 monounsaturated 18-carbon tail (Figure 1) which imparts a lower maximal level of inhibition at GlyT2 and may provide important clues for the future development of partial inhibitors.

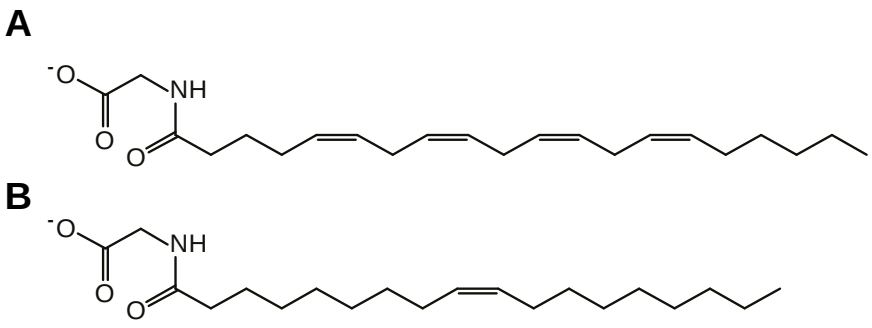


**Figure 1. Structures of N-arachidonyl glycine (NAGly) (A, compound 1) and N-oleoyl glycine (NOGly) (B, compound 2).**

Previous attempts to improve potency at GlyT2 lead our group to test commercially available acyl-carnitines and identified oleoyl L-carnitine (OLCarn) as a GlyT2 inhibitor with an $IC_{50}$ of 320 nM. Despite OLCarn having an increased potency compared to previous lipids its therapeutic effectiveness may be limited by its very slow offset as it has been suggested that irreversible inhibitors of GlyT2 are implicated in excitotoxicity. Furthermore, OLCarn is widely used as a shuttling molecule in the metabolism of lipids[25] and at high concentrations can cause disruptions to the integrity of cell membranes[24]. It is anticipated that modifying a scaffold of a known reversible inhibitor may produce more potent and partial inhibitors whilst maintaining reversibility and minimizing membrane disruption.

We have previously reported that compounds containing saturated or polyunsaturated tails are either inactive or have a much lower potency[24]. This is in contrast to N-acyl ethanolamine derivatives of anandamide where 3 or 4 double bonds were required to impart significant activity at CB receptors[12, 26, 27]. The tail group of the compounds contribute to the mechanism of inhibition, but the extent of its influence is unknown. In this study, we report the synthesis of glycine conjugated monounsaturated 14-, 16- or 18-carbon lipids and their potency in inhibiting glycine transport by GlyT2 and the closely related GlyT1 transporter.

## RESULTS AND DISCUSSION

NOGly (Figure 1) is comprised of a glycine head group covalently bonded to an 18 carbon monounsaturated fatty acid (MUFA) tail bearing an ω-9 *cis*-double bond (denoted in this paper as C18ω9 gly). To examine the influence of double bond position on GlyT2 inhibition, a series of NOGly analogues were synthesised in which the alkene bond was located at the ω-11, 7, 5 or 3 position. We also prepared analogues with ω-12 and 6 double bonds, which are common motifs in natural fatty acids, as well as both *cis*- and *trans*- isomers. In addition, acyl glycine compounds with 14- and 16-carbon MUFA tails were synthesised to assess the impact of chain length on potency.

### Chemistry

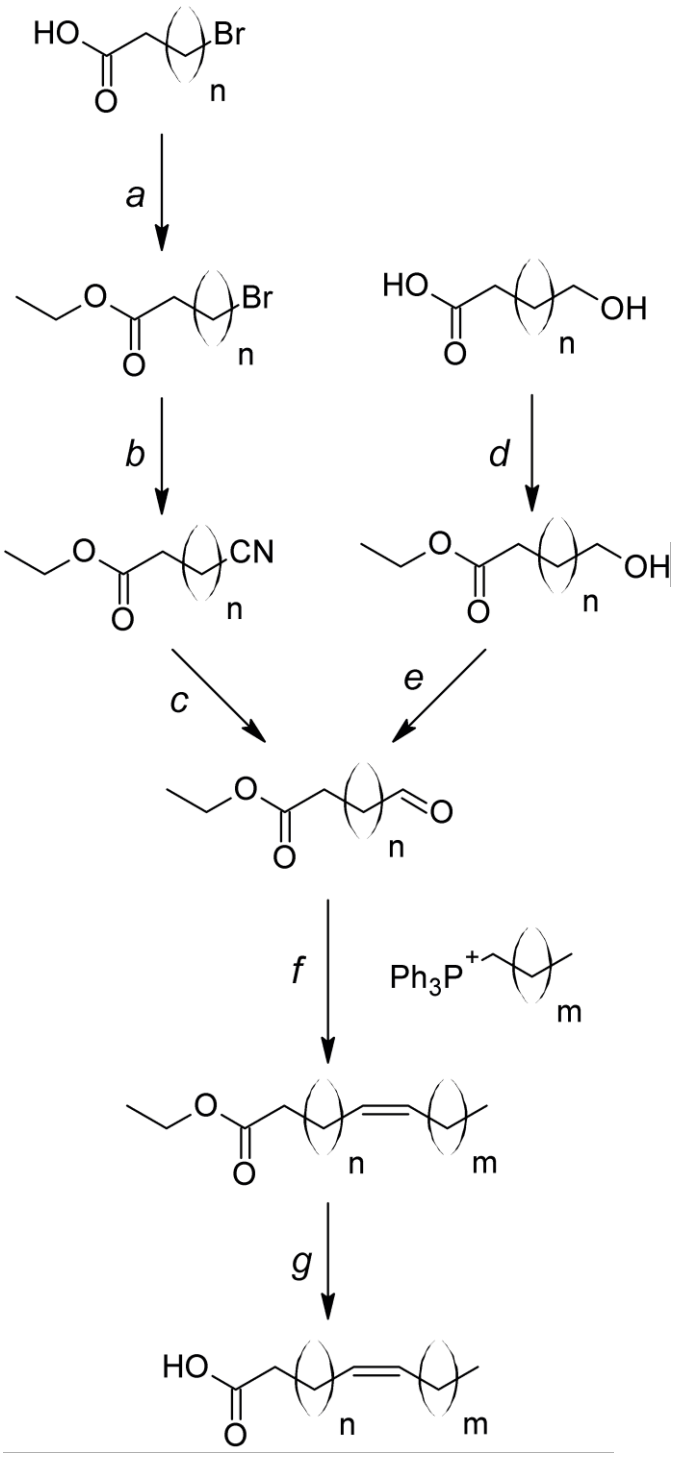


**Scheme 1. Synthesis of monounsaturated fatty acids (MUFAs).** *Reagents and conditions:* (a) ethanol, AcCl, rt, 4h; (b) NaCN, rt, 18h; (c) Raney Ni, NaH PO, 40 C, 2h; (d) ethanol, AcCl, rt, 4h; (e) PCC, 2h; (f) NaN(TMS)2, -78 C to rt, 2h; (g) NaOH, rt, 3 h.

MUFAs are key intermediates in the preparation of acyl glycine compounds **3 – 20**. Non-commercially available MUFAs were synthesised using our previously reported synthetic strategy[28] that utilizes the Wittig reaction of oxo-fatty acids with alkyl triphenylphosphonium bromide compounds (Scheme 1). The Wittig reaction provided excellent *cis*-stereoselectivity (*cis:trans* ≥ 97:3) and the flexibility to prepare MUFAs with different carbon chain lengths and double bond positions. For example, reaction of ethyl 12-oxododecanoate with the hexyl triphenylphosphonium bromide yielded, after removal of the ester protecting group, *cis*-octadec-12-enoic acid (a C18 ω-6 MUFA).

The procedure used to prepare the intermediate oxo-fatty acids was dependent on the commercial availability of starting materials (see Supporting Information for full details). The more facile synthesis utilized ω-hydroxy fatty acids, which were first esterified with acetyl chloride and ethanol (Scheme 1, step d) and then oxidised using pyridinium chlorochomate (PCC, step e). Due to the limited commercial availability of several hydroxy fatty acids, a second route to the oxo-fatty acids was developed whereby ω-bromo fatty acids were esterified (step a) and then reacted with NaCN (step b) to generate ω-nitrile intermediates. Selective reduction of the nitrile groups to aldehyde groups without concurrent reduction of the ester groups was achieved using Raney nickel and sodium hypophosphite (step c). Wittig reaction of the oxo-fatty acids with alkyl triphenyl phosphonium bromide compounds gave the MUFA esters (step f). The reactions were carried out in tetrahydrofuran with sodium bis(trimethylsilyl)amide at -78 $^{o}$C to promote *cis*-stereoselectivity. Base-catalysed hydrolysis of the resulting MUFA-esters (step g) yielded the desired MUFAs.

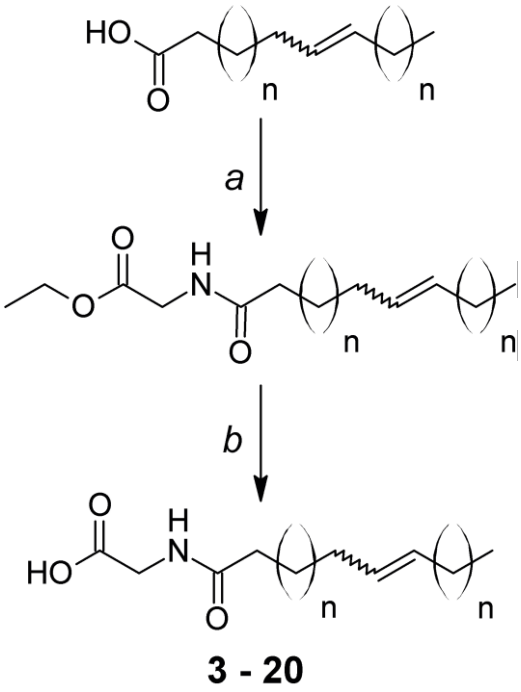


**Scheme 2 Synthesis of acyl glycine compounds 3 - 20.** *Reagents and conditions:* (a) EDCI, HOBt, glycine ethyl ester, $NEt_3$ , rt, 18h; (b) NaOH, rt, 3 h.

The acyl glycines **3** - **20** were prepared from the corresponding MUFAs in a two-step synthesis (Scheme 2). In the first step, amide bonds between the MUFAs and ethyl ester protected glycine were formed using the peptide coupling reagent N-ethyl-N′-(3-dimethylaminopropyl)carbodiimide hydrochloride (EDCI). Subsequent base-catalysed removal of the ester protecting group afforded compounds **3** - **20**.

## Critical Micelle Concentrations of acyl-glycines

The synthesized lipids are amphipathic with a hydrophobic aliphatic tail and a polar head group and have the propensity to spontaneously form micelles in solution at a characteristic critical micelle concentration (CMC). Thus, concentrations of lipids higher than the CMC may not freely diffuse to interact with proteins and thereby limit its biological activity. The CMC for OLCarn is approximately 7 µM [24] and 100 µM for NAGly[29]. Given the reduced charge of the acyl-glycines compared to the acyl-

carnitines, the CMCs of our novel lipids are likely to be significantly greater than that of OLCarn and so in all studies we limited the maximum concentration of lipids used to less than 30 µM, to minimise the possibility that partial inhibition is a consequence of lipid micelle formation limiting the available concentration and access of the lipid to the transporter. Thus, we suggest that for each of the novel acyl-glycine inhibitors that the degree of partial inhibition is a reflection of the way that the lipid interacts with the transporter. However, it should be noted that for NAGly (**1**), a true plateau of inhibition was not reached for concentrations less than its CMC. Curve fitting of this partial concentration response predicts full inhibition at higher concentrations. In the case of NAGly, the solubility of the compound could be limiting the level of inhibition reached in both *in vitro* and *in vivo* assays.

**Biological Activity**

Glycine transport by GlyT2a and GlyT1b is coupled to the co-transport of $3Na^+/1Cl^-$ and $2Na^+/1Cl^-$ respectively[17], creating an electrogenic process that can be measured electrophysiologically. Application of glycine to *Xenopus laevis* oocytes expressing GlyT2, clamped at -60 mV, results in inward currents with an $EC_{50}$ of 21.6 ± 1.6 µM, which is consistent with previously reported values[30]. The inhibitory profiles of each of the synthesised compounds was assayed by measuring glycine dependent ($EC_{50}$) currents in the presence of increasing concentrations of lipid to determine $IC_{50}$ values at GlyT2a and GlyT1b (herein referred to as GlyT2 and GlyT1).

NAGly (**1**) and NOGly (**2**) have previously been shown to be non-transportable, non-competitive inhibitors of GlyT2 with little or no activity on GlyT1[14, 24, 31]. The newly synthesized acyl-glycines do not generate any currents when applied to oocytes at concentrations up to 10 µM for 5 minutes, which are conditions that lead to a

substantial destabilising inward current when 3 µM OLCarn is applied[24]. The lack of any acyl-glycine induced current suggests that these compounds are not substrates for the transporter and also that the compounds are unlikely to induce any chaotropic effects on the cell membrane. Application of the $EC_{50}$ concentration of glycine produced robust inward currents (Figure 2), which were reduced in the presence of lipid inhibitors (representative current traces are shown for C16ω6 gly (**15**) and C18ω8 gly (**7**) inhibition of glycine transport). Following inhibition, glycine and inhibitor were washed from the bath by continuously perfusing recording buffer over the oocyte. Re-application of glycine five minutes post-inhibition results in currents comparable to pre-exposure glycine transport, indicating that binding of the inhibitors is reversible. Concentration inhibition curves were generated for each compound with the % max inhibition, and relative $IC_{50}$ values at GlyT2 and GlyT1 presented in Table 1. Whilst many compounds showed marked inhibition of transport by GlyT2, none of the compounds tested showed any appreciable inhibitory activity on the closely related glycine transporter GlyT1.

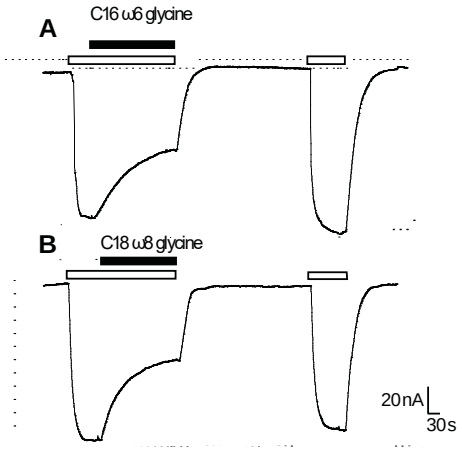


**Figure 2. Example current traces from oocytes expressing GlyT2 and clamped at -60 mV.** 30µM glycine was applied (open bars) and produced inward currents which were inhibited (closed bars) by 1 µM C16ω6 gly (15) and B. C18ω8 gly (7). Five minutes following inhibition the $EC_{50}$ of glycine was reapplied to show reversibility of inhibition and restoration of glycine currents to pre-exposure levels.

**Table 1: Structure-activity relationships of C14-, C16- and C18 glycine compounds at GlyT2 and GlyT1**

| 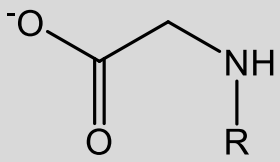 | | $IC_{50}$ (μM) (95 % CI) | | % max Inhibition of GlyT2[c] |
|---|---|---|---|---|
| | | GlyT2a | GlyT1b | |
| **Compound** | **R** | | | |
| **1** NAGly[a] | C20 *cis* ω6,9,12,15 | 9.1 (4.5-18) | >10[b] | 79.6 ± 2.08 |
| **2** NOGly[a] | C18 *cis* ω9 | 0.50 (0.23-1.1) | >10 | 66.8 ± 2.79 |
| **3** | C18 *cis* ω3 | >10 | >10 | - |
| **4** | C18 *cis* ω5 | >10 | >10 | - |
| **5** | C18 *cis* ω6 | >10 | >10 | - |
| **6** | C18 *cis* ω7 | >10 | >10 | - |
| **7** | C18 *cis* ω8 | 0.32 (0.18-0.57) | >10 | 61.3 ± 1.69 |
| **8** | C18 *cis* ω10 | 0.34 (0.14-0.84) | >10 | 52.4 ± 2.21 |
| **9** | C18 *cis* ω11 | >10 | >10 | - |
| **10** | C18 *cis* ω12 | >10 | >10 | - |
| **11** | C18 *trans* ω7 | >10 | >10 | - |
| **12** | C18 *trans* ω9 | >10 | >10 | - |
| **13** | C16 *cis* ω3 | 0.81 (0.46-1.4) | >10 | 65.3 ± 1.94 |
| **14** | C16 *cis* ω5 | 3.5 (2.8-4.4) | >10 | 92.3 ± 2.06 |
| **15** | C16 *cis* ω6 | 1.7 (1.4-2.2) | >10 | 85.2 ± 1.00 |
| **16** | C16 *cis* ω7 | 1.5 (1.3-1.8) | >10 | 92.5 ± 1.55 |
| **17** | C16 *cis* ω9 | 3.2 (2.7-3.9) | >10 | 88.2 ± 2.57 |
| **18** | C16 *cis* ω11 | 3.4 (2.5-4.8) | >10 | 97.9 ± 2.32 |
| **19** | C16 *cis* ω12 | 0.93 (0.41-2.2) | >10 | 48.5 ± 1.41 |
| **20** | C14 *cis* ω5 | 9.2 (7.3-12) | >10 | 100 ± 7.21 |

**C**ompounds were tested for inhibition of 30 μM glycine transport by GlyT2 and GlyT1, expressed in *Xenopus laevis* oocytes.. Measurements were taken from 2 batches of oocytes and at least 3 cells from each batch. Data presented are mean with 95% confidence intervals for each measurement (CI).

[a]Compounds are commercially available and have been previously described as GlyT2 inhibitors. [b]Where significant inhibition was not reached, $IC_{50}$ are presented as greater than the maximum concentration of each compound applied.
[c]Where a plateau in concentration-inhibition did not occur at the maximal concentration used the % max response given is the inhibition at the max concentration.

## Activity of C18 acyl-glycines

Maintaining the 18-carbon chain and positioning the double bond more than two bonds from the ω9 position (in compounds **3** – **6**, **9** and **10**), produced inactive compounds. To further probe this apparent strict requirement for double bond position we synthesised C18ω8 gly (**7**) and C18ω10 gly (**8**), in which the double bond is shifted by only one bond. Both analogues had slightly increased potencies compared to NOGly (0.32 for **7** and 0.34 μM for **8** compared to 0.50 μM for NOGly). It is notable that shifting the position of the double bond by one further carbon (C18ω7 (**6**) or C18ω11 (**9**)) to either end of the lipid chain abolished inhibitory activity (Figure 3). For the C18-compounds it is apparent that compounds with double bonds in this “goldilocks zone” are selective for GlyT2. It is also notable that these C18 acyl-glycine are partial inhibitors of GlyT2, with the maximal level of inhibition observed being 52-66% (Table 1).

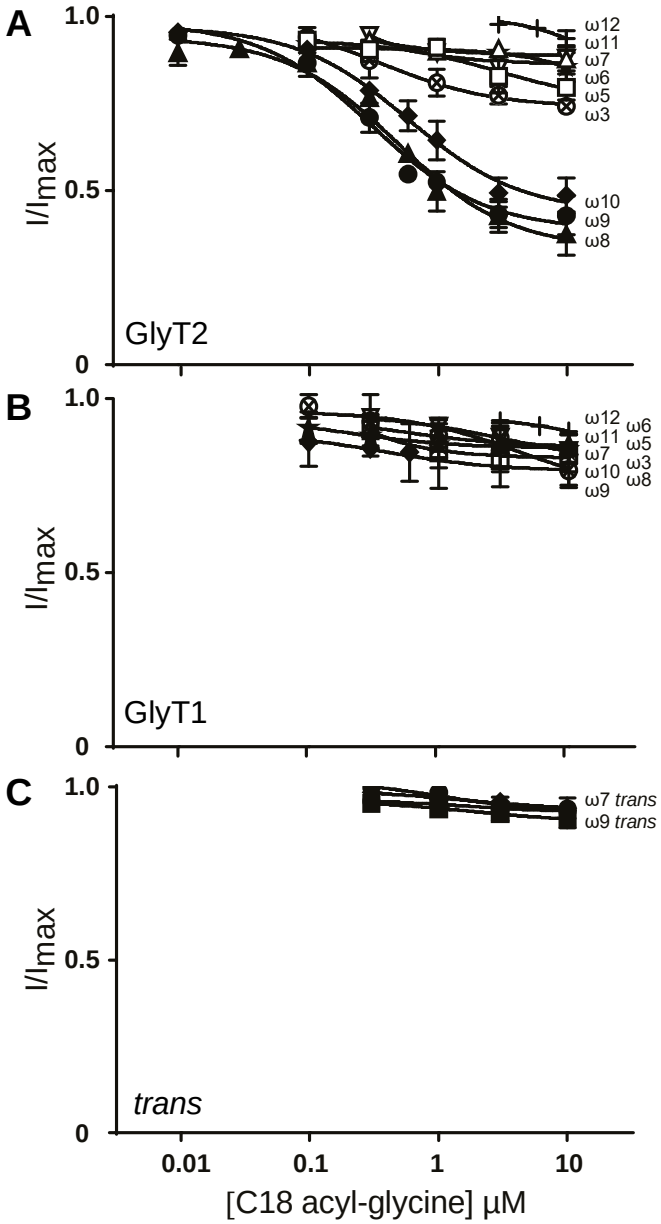


**Figure 3. Monounsaturated C18 acyl-glycines inhibit glycine transport currents of GlyT2 and GlyT1 transporters expressed in Xenopus laevis oocytes**. 30 µM glycine transport currents were measured in the presence of lipids (compounds 2-10 in Table 1) in the range of 10 nM to 10 µM for GlyT2 (A), GlyT1 (B). Concentration-dependent inhibition of GlyT2 and GlyT1 for compounds 11 and 12. The responses are normalised mean values ± SEM (n ≥ 3 cells) fit using least squares analysis.

Flexible monounsaturated lipids can exist in a number of different conformations. If the tail was not directly interacting with GlyT2, and instead sticking in the membrane or adjacent to hydrophobic regions of the transporter, a large number of subtle binding positions could be accommodated. To further probe the importance of the double

bond, *trans*- isomers of the ω7 and ω9C18- compounds were synthesised and screened on GlyT2 and GlyT1. The minimum energy conformation of a hydrocarbon tail with a *cis*- double bond approximately medial has a substantial kink, which has been shown to distort the packing of membrane lipids[31]. However, *trans*- double bonds would constrain the geometry of the tail to adopt a similar conformation as saturated lipids, which have been previously shown to be inactive at GlyT2[24]. In contrast to the *cis*- isomers, C18*trans*- ω9 gly (**12**) and C18*trans*- ω7 gly (**11**) were both inactive which suggests there is a selective pocket on GlyT2 which can only accommodate *cis*- conformations of the lipid tail moiety.

**Activity of the C16 and C14 acyl-glycines**

Substitution of the lipid tail in NAGly with C16-MUFAs and a double bond at any of the ω3, ω5, ω6, ω7, ω9, ω11, or ω12 positions, produced compounds which were active at GlyT2 with $IC_{50}$ values ranging from 0.81 to 3.5 µM (Figure 4). As can be seen by the % max inhibition (Table 1), a majority of the C16- compounds inhibited glycine transport currents to a greater extent than previously reported lipid inhibitors of GlyT2. C16- compounds with double bonds in the ω5 through ω11 positions inhibited GlyT2 in the range of 85 – 98% (Table 1). Shortening the chain also appeared to reduce the affinity of the acyl-glycines (C14ω5 gly $IC_{50}$ 9.2 µM).

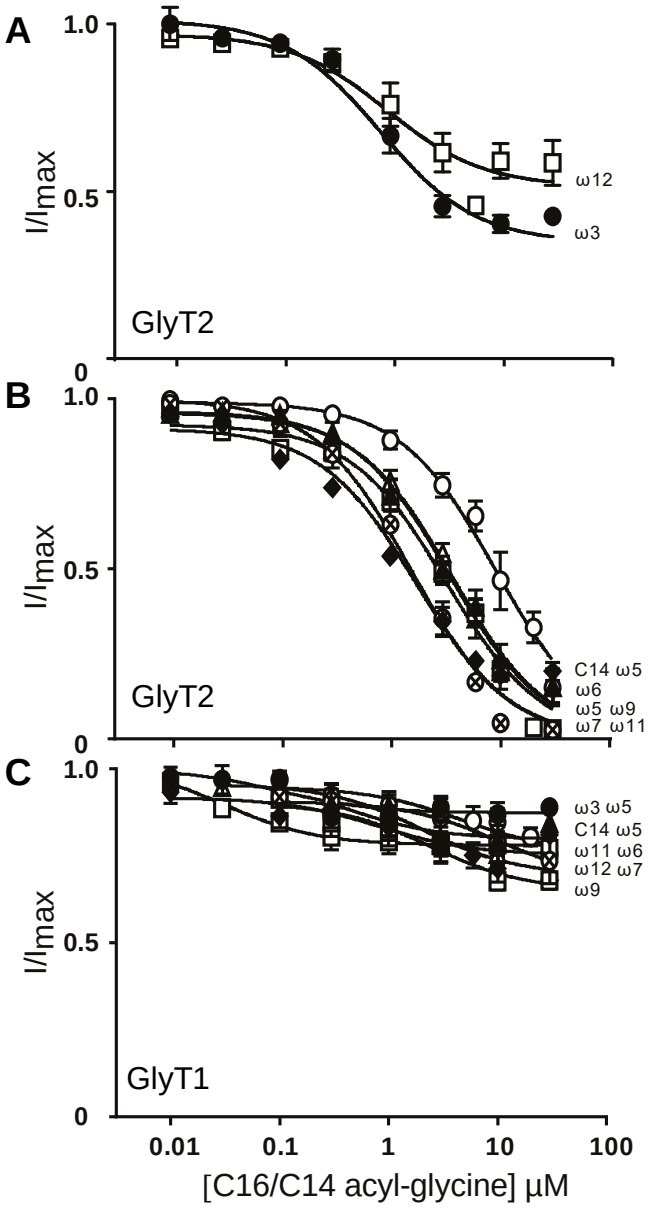


**Figure 4. Monounsaturated C16 and C14 acyl-glycines inhibit glycine transport currents of GlyT2 and GlyT1 transporters expressed in Xenopus laevis oocytes**. 30 µM glycine transport currents were measured in the presence of lipids in the range of 10 nM to 10 µM. A. Concentration-inhibition curves for partial inhibitors (compounds 13 and 19 (see Table 1)) on GlyT2 B. Concentration-inhibition curves for full inhibitors (Compounds 14-18, and 20) on GlyT2. C. Concentration-dependent effects of compounds 13-20 on glycine transport currents of GlyT1. The responses are normalised mean values ± SEM (n ≥ 3 cells) fit using least squares analysis.

**Acyl-Glycines Inhibit $^{3}$H-Glycine uptake by oocytes expressing GlyT2.**

Whilst it has been previously demonstrated that glycine-induced currents are directly related to the rate of glycine transport, we also checked that representative lipids also inhibit the rate of $^{3}$H-glycine uptake by oocytes expressing GlyT2. A time course of $^{3}$H-Glycine uptake was measured in the absence of inhibitors and also in the presence of 10 μM C18ω8 Gly and 10 μM C16ω3 Gly and also compared to 1 μM ALX1393. Both lipids caused ~50% reductions in the rate of $^{3}$H-Glycine transport over 10 minutes (Figure 5), which are comparable to the effects observed for inhibition of glycine transport currents. It is notable that uninjected oocytes allowed ~15% of uptake compared to oocytes expressing GlyT2 and that this background level of uptake was not affected by the acyl-glycines. Thus, the lack of any substantial change in the rate of background $^{3}$H-Glycine uptake also confirms that there is minimal, if any, chaotropic effects of the lipids on the cell membrane.

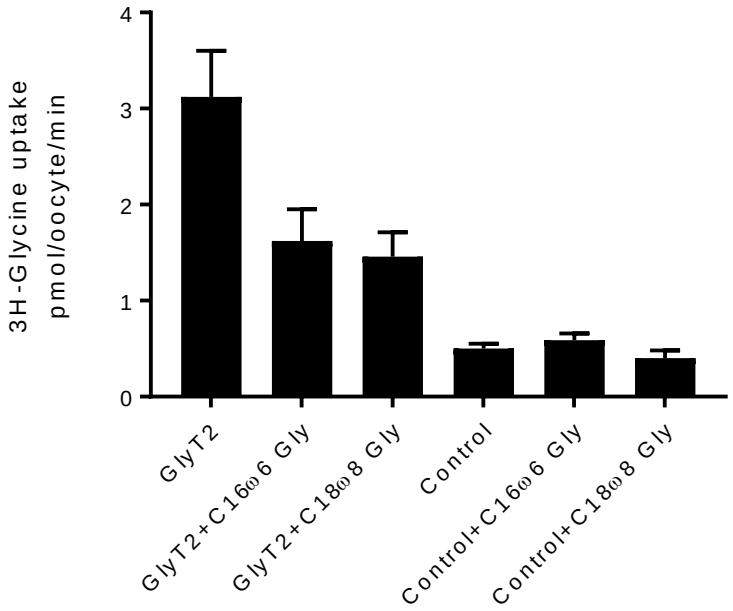

**Figure 5: Rates of $^{3}$H-Glycine uptake in the presence and absence of acyl-glycine inhibitors.** Oocytes expressing GlyT2 and uninjected control oocytes were preincubated with 10 μM C16ω6 Gly, 10 μM C18ω8 or buffer for 2 minutes and then the rate of 10 μM $^{3}$H-glycine transport measured as described in the methods.

## There is a preferred double bond position and chain length for conferring affinity and extent of inhibition

It appears that when the double bond is in the centre of the carbon chain, the inhibitors are active (in the case of C18) or show a greater level of maximal inhibition (in the case of C16). However, as the properties imparted by a medial double bond differ between C16- and C18- compounds it cannot be ascertained whether the trend is connected. The order of potency was C18 > C16 > C14 for the monounsaturated compounds tested, which suggests tail length is governing activity of the inhibitors. While C18- compounds were the most potent, the placement of the double bond within the tail was limited to a stringently defined zone in the middle of the chain. The lower affinity C14- and C16- compounds were all active as GlyT2 inhibitors, with generally increased maximal level of inhibition. Whilst the C18 compounds are more potent than their C16 counterparts, the maximal level of inhibition was reduced (52-67% for C18ω8, 9, 10, and 88-92% for C16ω5, 6, 7, 9, 11). We speculate that there is an optimal size and/or shape of tails which can be accommodated in the allosteric inhibitor binding pocket. Whilst lipids with C14, C16 and C18 tails with glycine head group can fit into a binding pocket, lipids with larger C18 tails are likely to have the potential to form more hydrophobic interactions causing increased potency of inhibition, but also creating partial inhibitors. In the case of NAGly, its longer polyunsaturated tail would be more condensed than the shorter monounsaturated lipids, allowing it to fit in the lipid binding site. The observed lower affinity of NAGly

could be due to the number of kinks in the tail which restrict the ideal binding mode and reduce the capacity for intermolecular interactions.

The majority of mammalian cell membranes are composed of phosphatidylcholine (PC), with phosphatidylethanolamine (PE), sphingomyelin, and cholesterol also abundantly present[32]. Unsaturated C18- or saturated C16- are the most common lipid chains present in PC and PE. The most efficacious of the lipid inhibitors in this study contain similar tails and therefore may be capable of inserting into the bilayer and interacting with or displacing membrane lipids at the protein membrane interface. It has been suggested that ligands may access the binding site of CB receptors via the cell membrane[7]. Molecular dynamics simulations of the endogenous cannabinoid *sn*-2-arachidonylglycerol (2-AG) with a typical PC bilayer observe the 2-AG lipid first associating with the membrane phospholipids, followed by migration of 2-AG to interact with the $CB_2$ receptor[6]. 2-AG then enters the ligand binding site by moving through an opening between membrane exposed helices VI and VII. In the recent crystal structure of the antagonist bound $CB_1$ receptor[34], hydrophobic residues in helices II, III, VI, and VII comprised part of the antagonist binding site which was also the site of hydrophobic tail interactions with anandamide and 2-AG in subsequent docking. The lipid inhibitors of GlyT2 may also sit in the membrane parallel to the membrane phospholipids spanning the depth of one leaflet. The predilection for certain tail lengths and configurations may also reflect the capacity for the acyl-glycines to associate with the membrane and form a lipid-bound pool. Acyl-glycines could then inhibit GlyT2 by channelling through membrane-exposed transmembrane helices in a similar manner predicted for the cannabinoid

ligands and the lipid inhibitor ML056 on the sphingosine-1-phosophate receptor ($S1P_1R$)[35].

Other arachidonyl lipids have been shown to modulate ion channels either by increasing function[36] or as an inhibitor[3]; for example, arachidonic acid is an open channel blocker of $hK_v1.5$ with an $IC_{50}$ of 6.1 μM[3]. Studies of the structure-activity relationship for lipid ligands of CB receptors have also revealed that small changes can impart inactivity[7, 26, 27, 37]. NAGly and anandamide differ only by a carboxylic acid in the head group and yet this difference is sufficient to prevent binding of NAGly. The acyl-glycines in this study have a preferred double bond position and chain length which, in addition to the well characterised importance of the head group, establishes the coinciding influence of the tail in conferring the activity of lipid ligands.

**Potency is not driving the reversibility of inhibition**

Following a 5 minute washout of each of the active inhibitors, glycine transport currents were comparable to the pre-lipid exposure transport currents (Figure 2). Despite the differences in lipid tail, and large variation in relative potency (0.32-9.2 μM), all inhibitors in this study were reversible. These observations are in contrast to oleoyl L-carnitine inhibition of GlyT2 which is very slowly reversible[24]. This suggests that the head group is more important in determining the rate of reversibility. The $IC_{50}$ of oleoyl L-carnitine is similar to the most potent acyl-glycine inhibitor (~320 nM) and so reversibility is not simply a reflection of the binding and unbinding rates from the transporter, and must be governed by some other mechanism. In the case of oleoyl L-carnitine, application of β-cyclodextrin accelerates washout[24] which suggests that it is a lipid membrane-mediated mechanism of inhibition. Thus, we speculate that the head group influences the stability of the lipid in the membrane, which can influence the time course of washout of the lipid.

Since neither potency at the binding site nor hydrophobic interactions of the tail in the membrane are driving reversibility, we propose that reversibility is related to how compounds can access or leave the site and therefore is another independent property of the compound that must be considered when designing an optimal GlyT2 lipid inhibitor. A carnitine head group has a positive charge and is significantly larger than the glycine head group, so perhaps the charge and/or size is capturing the compounds in a membrane reservoir, such as the negatively charged phosphate groups of the lipid bilayer, for longer periods impeding washout.

In addition to full inhibition, reversibility is another potential problem which is hindering the pursuit of GlyT2 as a molecular target. The excitotoxicity of ORG-25543 is associated with both its full and irreversible inhibition[21] and it has been suggested that instead a reversible inhibitor may be used to avoid adverse side effects. As all inhibitors identified in this study are readily reversible within 5 minutes it is promising that they will be efficacious and without side effects.

## CONCLUSIONS

A number of crystal structures of neurotransmitter transporters with the conserved LeuT-like fold show lipids interacting with the protein[2,38], but the extent that lipid interactions may impact on the function of the transporters is not well understood. We have demonstrated that the lipid constituent of acyl-glycine compounds is essential in their specific interactions and mechanism of inhibition of the LeuT-like transporter, GlyT2, and not merely a non-selective, “sticky” adjunct. The data presented here establishes there is an ideal chain length and double bond conformation, and that potency and maximal level of inhibition are influenced by the lipid tail. Conservative differences between compounds are sufficient to impart or

remove inhibitory activity which validates highly specific binding to a subtype selective allosteric pocket. In order to better understand the structural basis for lipid-protein interactions and provide a working hypothesis for the requirements of double bonds in the acyl-tail, the specificity of acyl-head group interactions, and the molecular determinants for partial inhibition a comprehensive mutagenesis approach and/or structural studies will be required.

In this study we have synthesized a number of acyl-glycine compounds which are GlyT2 inhibitors and contain novel synthetic tails which may be less susceptible to enzymatic degradation than the parent compound NAGly. We have identified a relatively potent (320 nM), reversible, and partial (61 ± 1.7 %) novel inhibitor of GlyT2 which has low activity on GlyT1 and is ~28-*fold* more potent than the endogenously produced ligand, NAGly. We suggest that partial inhibitors may have an advantage over full inhibitors by slowing the rate of clearance of glycine from the synapse rather than stopping it completely. Whilst this mechanism of inhibition should allow prolonged signalling through postsynaptic and extrasynaptic glycine receptors, it should not disrupt the equilibrium cytosolic glycine concentration and thereby allow maintenance of glycine vesicle filling and subsequent synaptic glycine release[19]. A greater understanding of what governs the inhibitory properties of acyl-glycine compounds may spur the development of effective GlyT2 inhibitors with desired maximal inhibition and reversibility characteristics, a complication which has hampered the progress of GlyT2 inhibitors as therapeutics.

## METHODS

### General Chemistry

(*Z*)-hexadec-13-enoic acid and (*Z*)-octadec-15-enoic acid were prepared by our previously reported procedures [39,40]. (*E*)-octadec-9-enoic acid was purchased from Chemsupply (Gillman, SA, Australia). (*Z*)-hexadec-9-enoic acid, (*Z*)-octadec-11-enoic acid, (*E*)-octadec-11-enoic acid, (*Z*)-octadec-6-enoic acid and all other reagents and anhydrous solvents were purchased from Sigma Aldrich (Castle Hill, NSW, Australia). Non-commercially available MUFAs were synthesised as described in the supporting information. The purity of all test compounds (**3** – **20**) was confirmed by elemental analysis carried out in the Campbell Microanalytical Laboratory at the Department of Chemistry, University of Otago. All values were within ±0.4% of the calculated values. Dry Column Vacuum Chromatography (DCVC) was used to purify reaction products on silica gel with gradient elutions. TLC was performed on silica gel 60 $F_{254}$ plates. $^{1}H$ and $^{13}C$ NMR spectra were recorded on an Agilent 500 MHz NMR. Spectra were referenced internally to residual solvent ($CDCl_3$; $^{1}H$ $\delta$ 7.26, $^{13}C$ $\delta$ 77.10. $d_6$-DMSO; $^{1}H$ $\delta$ 2.49, $^{13}C$ $\delta$ 39.52). High resolution mass spectra were recorded on Agilent 6510 Q-TOF LC/MS.

### General procedure for EDCI coupling reaction

To a solution of MUFA (2.0 mmol) in anhydrous DMF (10 mL) was added hydroxybenzotriazole hydrate (2.40 mmol), and EDCI (2.80 mmol). The mixture was stirred at room temperature for 1 h, then glycine ethyl ester hydrochloride (1.0 mmol) and triethylamine (0.607 g, 6.0 mmol) were added. The reaction mixture was stirred for 18 h, then diluted with water (50 mL). The crude product was extrated with ethyl

acetate (3 x 25 mL) and purified on silica gel by stepwise gradient elution with chloroform/isopropanol (100:0 to 90:10), yielding the products as white solids.

**ethyl 2-[[(Z)-octadec-15-enoyl]amino]acetate.** Yield = 93%, white powder. Mp. = 49 - 51 $^{o}$C. $^{1}$H NMR (500 MHz, $CDCl_3$) δ 5.92 (s, 1H), 5.40–5.30 (m, 2H), 4.22 (q, *J*=7.0Hz, 2H), 4.04 (d, *J*=5.5Hz, 2H), 2.24 (t, *J*=7.5Hz, 2H), 2.08-1.95 (m, 4H), 1.65 (p, *J*=7.0Hz, 2H), 1.35-1.20 (m, 23H), 0.89 (t, *J*=7.5Hz, 3H). $^{13}$C NMR (100 MHz, $CDCl_3$): δ 173.20, 170.17, 131.40, 129.32, 61.50, 41.31, 36.44, 29.76, 29.59, 29.57, 29.51, 29.44, 29.39, 29.33, 29.30, 29.27, 29.21, 27.10, 25.60, 20.46, 14.39, 14.12. HRMS (ESI) *m/z* $[M+H]^+$ calcd for $C_{22}H_{42}NO_3$, 368.3159; found, 368.3162.

**ethyl 2-[[(Z)-octadec-13-enoyl]amino]acetate.** Yield = 90%, white powder. Mp. = 46 - 47 $^{o}$C. $^{1}$H NMR (500 MHz, DMSO-$d_6$) δ 8.18 (t, *J*=6.0Hz, 1H), 5.32–5.30 (m, 2H), 4.06 (q, *J*=7.0Hz, 2H), 3.76 (d, *J*=6.0Hz, 2H), 2.10 (t, *J*=7.5Hz, 2H),1.99-1.95 (m, 4H), 1.46 (*p*, *J*=7.0Hz, 2H), 1.30-1.23(m, 20H), 1.17(t, *J*=7.0Hz, 3H), 0.84 (t, *J*=7.0Hz, 3H). $^{13}$C NMR (100 MHz, DMSO-$d_6$): δ 172.92, 170.19, 129.83, 129.79, 60.48, 40.81, 35.19, 31.56, 29.28, 29.19 (3C), 29.17, 29.12, 29.04, 28.99, 28.76, 28.73, 26.75,26.50, 25.37, 21.91, 14.25, 14.00. HRMS (ESI) *m/z* $[M+H]^+$ calcd for $C_{22}H_{42}NO_3$, 368.3159; found, 368.3157.

**ethyl 2-[[(Z)-octadec-12-enoyl]amino]acetate.** Yield = 76%, white powder. Mp. = 48 - 49 $^{o}$C. $^{1}$H NMR (500 MHz, DMSO-$d_6$) δ 8.19 (t, *J*=6.0Hz, 1H), 5.35–5.33 (m, 2H), 4.21 (q, *J*=7.0Hz, 2H), 3.76 (d, *J*=5.5Hz, 2H, 2H), 2.20 (t, *J*=7.5Hz, 2H), 2.04-1.99 (m, 4H), 1.46 (*p*, *J*=7.0Hz, 2H), 1.30-1.23 (m, 20H), 1.17 (t, *J*=7.0Hz, 3H), 0.88 (t, *J*=7.0Hz, 3H) . $^{13}$C NMR (100 MHz, DMSO-$d_6$): δ 173.23, 170.16, 129.91, 129.88, 61.52, 41.34, 36.46, 31.53, 29.77, 29.57,.29.52, 29.46, 29.48, 29.34, 29.30, 29.25, 27.20, 27.17,

25.58, 22.58, 14.14, 14.08. HRMS (ESI) *m/z* $[M+H]^+$ calcd for $C_{22}H_{42}NO_3$, 368.3159; found, 368.3153.

**ethyl 2-[[(Z)-octadec-11-enoyl]amino]acetate.** Yield = 77%, white powder. Mp. = 48 - 49 °C. $^1$H NMR (500 MHz, DMSO-$d_6$) δ 8.18 (t, *J*=6.0Hz, 1H), 5.32–5.30 (m, 2H), 4.06 (q, *J*=7.0Hz, 2H), 3.76 (d, *J*=6.0Hz, 2H, 2H), 2.10(t, *J*=7.5Hz, 2H), 2.00-1.95(m, 4H), 1.46 (*p*, *J*=7.0Hz, 2H), 1.30-1.23(m, 20H), 1.17(t, *J*=7.0Hz, 3H), 0.84 (t, *J*=7.0Hz, 3H) . $^{13}$C NMR (100 MHz, DMSO-$d_6$): δ 175.81, 173.11, 132.76(2C), 63.39, 43.73, 38.12, 34.25, 32.24, 32.21, 32.05, 31.97, 31.92, 31.72, 31.67, 31.39, 29.72, 29.70, 28.30, 25.21, 17.18, 17.05. HRMS (ESI) *m/z* $[M+H]^+$ calcd for $C_{22}H_{42}NO_3$, 368.3159; found, 368.3159.

**ethyl 2-[[(Z)-octadec-10-enoyl]amino]acetate.** Yield = 72%, white powder. Mp. = 48 - 49 °C. $^1$H NMR (500 MHz, DMSO-$d_6$) δ 8.18 (t, *J*=6.0Hz, 1H), 5.32–5.30 (m, 2H), 4.05 (q, *J*=7.0Hz, 2H), 3.76 (d, *J*=6.0Hz, 2H, 2H), 2.10 (t, *J*=7.5Hz, 2H), 2.00-1.95 (m, 4H), 1.47 (*p*, *J*=7.5Hz, 2H), 1.30-1.23 (m, 20H), 1.17 (t, *J*=7.0Hz, 3H), 0.84 (t, *J*=7.0Hz, 3H) . $^{13}$C NMR (100 MHz, DMSO-$d_6$): δ 172.68, 169.99, 129.64, 129.63, 60.27, 40.60, 34.98, 31.27, 29.11, 29.10, 28.79, 28.59, 28.54, 28.53, 26.59, 26.56, 25.17, 22.07, 20.76, 14.09, 14.06, 13.94. HRMS (ESI) *m/z* $[M+H]^+$ calcd for $C_{22}H_{42}NO_3$, 368.3159; found, 368.3159.

**ethyl 2-[[(Z)-octadec-8-enoyl]amino]acetate.** Yield = 73%, white powder. Mp. = 49 - 50 °C. $^1$H NMR (500 MHz, DMSO-$d_6$) δ 8.19 (t, *J*=6.0Hz, 1H), 5.32–5.30 (m, 2H), 4.07 (q, *J*=7.0Hz, 2H), 3.77 (d, *J*=6.0Hz, 2H, 2H), 2.10 (t, *J*=7.5Hz, 2H), 2.00-1.95 (m, 4H), 1.47 (*p*, *J*=7.5Hz, 2H), 1.28-1.20 (m, 20H), 1.17 (t, *J*=7.0Hz, 3H), 0.84 (t, *J*=7.0Hz, 3H) . $^{13}$C NMR (100 MHz, DMSO-$d_6$): δ 172.66, 170.98, 129.65, 129.61, 60.26, 40.60, 34.96, 31.27, 29.06, 29.04, 28.97, 28.86, 28.67(2C), 28.57, 28.41, 26.59, 26.56, 25.14,

21.02, 14.06, 13.95. HRMS (ESI) *m/z* $[M+H]^+$ calcd for $C_{22}H_{42}NO_3$, 368.3159; found, 368.3158.

**ethyl 2-[[(Z)-octadec-7-enoyl]amino]acetate.** Yield = 84%, white powder. Mp. = 48 - 49 °C. $^1$H NMR (500 MHz, DMSO-$d_6$) δ 8.20 (t, *J*=6.0Hz, 1H), 5.32–5.30 (m, 2H), 4.06 (q, *J*=7.5Hz, 2H), 3.76 (d, *J*=6.0Hz, 2H, 2H), 2.10 (t, *J*=7.0Hz, 2H), 1.99-1.95 (m, 4H), 1.48 (*p*, *J*=7.0Hz, 2H), 1.31-1.23 (m, 20H), 1.17 (t, *J*=7.0Hz, 3H), 0.88 (t, *J*=7.0Hz, 3H) . $^{13}$C NMR (100 MHz, DMSO-$d_6$): δ 174.06, 129.37 (2C), 60.18, 40.60, 34.39, 29.93, 29.56, 29.52, 29.51(2C), 29.48, 29.39(2C), 29.25, 29.22, 29.11, 26.82, 26.75, 24.96, 14.22, 14.05. HRMS (ESI) *m/z* $[M+H]^+$ calcd for $C_{22}H_{42}NO_3$, 368.3159; found, 368.3354.

**ethyl 2-[[(Z)-octadec-6-enoyl]amino]acetate.** Yield = 64%, white powder. Mp. = 47 - 48 °C. $^1$H NMR (500 MHz, DMSO-$d_6$) δ 8.19 (t, *J*=6.0Hz, 1H), 5.35–5.33 (m, 2H), 4.06 (q, *J*=7.5Hz, 2H), 3.76 (d, *J*=6.0Hz, 2H, 2H), 2.10 (t, *J*=7.0Hz, 2H), 1.99-1.95 (m, 4H), 1.48 (*p*, *J*=7.0Hz, 2H), 1.30-1.22 (m, 20H), 1.17 (t, *J*=7.0Hz, 3H), 0.84 (t, *J*=7.0Hz, 3H) . $^{13}$C NMR (100 MHz, DMSO-$d_6$): δ 173.07, 170.43, 130.24, 129.86, 60.73, 41.07, 35.31, 31.75, 29.58, 29.49, 29.47, 29.45, 29.34, 29.15, 29.11, 29.08, 27.07, 26.90, 25.29, 22.55, 14.52, 14.41. HRMS (ESI) *m/z* $[M+H]^+$ calcd for $C_{22}H_{42}NO_3$, 368.3159; found, 368.3155

**ethyl 2-[[(E)-octadec-11-enoyl]amino]acetate.** Yield = 90%, white powder. Mp. = 49 - 50 °C. $^1$H NMR (500 MHz, DMSO-$d_6$) δ 8.18 (t, *J*=6.0Hz, 1H), 5.35–5.30 (m, 2H), 4.06 (q, *J*=7.0Hz, 2H), 3.76 (d, *J*=6.0Hz, 2H, 2H), 2.09 (t, *J*=7.5Hz, 2H), 1.98-1.88(m, 4H), 1.47 (*p*, *J*=7.0Hz, 2H), 1.32-1.20 (m, 20H), 1.17 (t, *J*=7.0Hz, 3H), 0.84 (t, *J*=7.0Hz, 3H) . $^{13}$C NMR (100 MHz, DMSO-$d_6$): δ 175.81, 173.11, 132.76 (2C), 63.39, 43.73, 38.12, 34.25, 32.24, 32.21, 32.05, 31.97, 31.92, 31.72, 31.67, 31.39, 29.72, 29.70,

28.30, 25.21, 17.18, 17.05. HRMS (ESI) *m/z* $[M+H]^+$ calcd for $C_{22}H_{42}NO_3$, 368.3159; found, 368.3158.

**ethyl 2-[[(E)-octadec-9-enoyl]amino]acetate.** Yield = 90%, white powder. Mp. = 62 - 63 $^oC$. $^1H$ NMR (500 MHz, DMSO-$d_6$) δ 8.18(t, *J*=6.0Hz, 1H), 5.36–5.34 (m, 2H), 4.06(q, *J*=7.0Hz, 2H), 3.76(d, *J*=6.0Hz, 2H, 2H), 2.09(t, *J*=7.5Hz, 2H), 1.94- 1.91 (m, 4H), 1.47 (*p*, *J*=7.0Hz, 2H), 1.30-1.23(m, 20H), 1.17(t, *J*=7.0Hz, 3H), 0.84 (t, *J*=7.0Hz, 3H) . $^{13}C$ NMR (100 MHz, DMSO-$d_6$): δ 172.86, 170.16, 130.23 (2C), 60.44, 40.78, 35.15, 32.11, 31.43, 29.16 , 29.15, 28.98 (2C), 28.85, 28.80, 28.65, 28.56 (2C), 25.33, 22.25, 14.23, 14.11. HRMS (ESI) *m/z* $[M+H]^+$ calcd for $C_{22}H_{42}NO_3$, 368.3159; found, 368.3155.

**ethyl 2-[[(Z)-hexadec-13-enoyl]amino]acetate.** Yield = 87%, colourless liquid. $^1H$ NMR (500 MHz, $CDCl_3$) δ 5.92 (s, 1H), 5.40–5.30 (m, 2H), 4.22 (q, *J*=7.0Hz, 2H), 4.02 (d, *J*=5.5Hz, 2H), 2.23 (t, *J*=7.5Hz, 2H), 2.08-1.95 (m, 4H), 1.64 (p, *J*=7.0Hz, 2H), 1.35-1.20 (m, 19H), 0.96 (t, *J*=7.5Hz, 3H). $^{13}C$ NMR (100 MHz, $CDCl_3$): δ 173.21, 170.13, 131.45, 129.33, 61.51, 41.33, 36.45, 29.76, 29.58, 29.57, 29.51, 29.44, 29.31, 29.27, 29.24, 27.08, 25.56, 20.48, 14.38, 14.12. HRMS (ESI) *m/z* $[M+H]^+$ calcd for $C_{20}H_{38}NO_3$, 340.2846; found, 340.2840.

**ethyl 2-[[(Z)-hexadec-11-enoyl]amino]acetate.** Yield = 66%, colourless liquid. $^1H$ NMR (500 MHz, DMSO-$d_6$) δ 8.18 (t, *J*=6.0Hz, 1H), 5.33–5.31 (m, 2H), 4.07 (q, *J*-7.0Hz, 2H), 3.76 (d, *J*-6.0Hz, 2H), 2.09 (t, *J*=7.5Hz, 2H), 1.98-1.95 (m, 4H), 1.46 (*p*, *J*=7.0Hz, 2H), 1.28-1.23 (m, 16H), 1.16 (t, *J*=7.0Hz, 3H), 0.88 (t, *J*=7.0Hz, 3H) . $^{13}C$ NMR (100 MHz, DMSO-$d_6$): δ 172.87, 170.16, 129.80, 129.77, 60.44, 40.78, 35.16, 31.53, 29.28, 29.08, 29.00, 28.95, 28.75, 28.70, 26.74, 26.47, 25.34, 21.88, 14.23, 13.98. HRMS (ESI) *m/z* $[M+H]^+$ calcd for $C_{20}H_{38}NO_3$, 340.2846; found, 340.2847.

**ethyl 2-[[(Z)-hexadec-10-enoyl]amino]acetate.** Yield = 71%, colourless liquid. $^{1}$H NMR (500 MHz, DMSO-$d_6$) δ 8.18 (t, *J*=6.0Hz, 1H), 5.35–5.33 (m, 2H), 4.06 (q, *J*=7.0Hz, 2H), 3.76 (d, *J*=5.5Hz, 2H), 2.09 (t, *J*=7.5Hz, 2H), 1.99-1.95 (m, 4H), 1.46 (*p*, *J*=7.0Hz, 2H), 1.30-1.23 (m, 16H), 1.17(t, *J*=7.0Hz, 3H), 0.84 (t, *J*=7.0Hz, 3H) . $^{13}$C NMR (100 MHz, DMSO-$d_6$): δ 172.87, 170.16, 129.64, 129.45, 60.44, 40.75, 35.13, 31.50, 29.28, 29.08, 28.99, 28.95, 28.75, 28.70, 26.70, 26.43, 25.34, 21.85, 14.23, 13.98. HRMS (ESI) *m/z* $[M+H]^+$ calcd for $C_{20}H_{38}NO_3$, 340.2846; found, 340.2846.

**ethyl 2-[[(Z)-hexadec-9-enoyl]amino]acetate.** Yield = 65%, colourless liquid. $^{1}$H NMR (500 MHz, DMSO-$d_6$) δ 8.15 (t, *J*=6.0Hz, 1H), 5.29–5.27 (m, 2H), 4.05 (q, *J*=7.0Hz, 2H), 3.74 (d, *J*=5.5Hz, 2H), 2.07 (t, *J*=7.5Hz, 2H), 1.96-1.92 (m, 4H), 1.45 (*p*, *J*=7.0Hz, 2H), 1.27-1.21(m, 16H), 1.15 (t, *J*=7.0Hz, 3H), 0.82 (t, *J*=7.0Hz, 3H) . $^{13}$C NMR (100 MHz, DMSO-$d_6$): δ 172.78, 170.12, 129.75, 129.69, 60.41, 40.75, 34.78, 31.43, 29.27, 29.10, 29.00, 28.84, 28.78, 28.37, 26.76, 26.72, 25.21, 22.24, 14.22, 14.11. HRMS (ESI) *m/z* $[M+H]^+$ calcd for $C_{20}H_{38}NO_3$, 340.2846; found, 340.2850.

**ethyl 2-[[(Z)-hexadec-7-enoyl]amino]acetate.** Yield = 63%, colourless liquid. $^{1}$H NMR (500 MHz, DMSO-$d_6$) δ 8.18 (t, *J*=6.0Hz, 1H), 5.32–5.30 (m, 2H), 4.06 (q, *J*=7.0Hz, 2H), 3.77 (d, *J*=6.0Hz, 2H), 2.09 (t, *J*=7.5Hz, 2H), 1.97-1.95 (m, 4H), 1.48 (*p*, *J*=7.5Hz, 2H), 1.30-1.23 (m, 16H), 1.17 (t, *J*=7.0Hz, 3H), 0.84 (t, *J*=7.0Hz, 3H) . $^{13}$C NMR (100 MHz, DMSO-$d_6$): δ 172.78, 170.12, 129.79, 129.69, 60.41, 40.75, 35.10, 31.43, 29.27, 29.10, 29.00, 28.84, 28.78, 28.37, 26.74, 26.71, 25.21, 22.24, 14.20, 14.08. HRMS (ESI) *m/z* $[M+H]^+$ calcd for $C_{20}H_{38}NO_3$, 340.2846; found, 340.2850.

**ethyl 2-[[(Z)-hexadec-5-enoyl]amino]acetate.** Yield = 50%, colourless liquid. $^{1}$H NMR (500 MHz, DMSO-$d_6$) δ 8.20 (t, *J*=5.5Hz, 1H), 5.34–5.30 (m, 2H), 4.06 (q, *J*=7.0Hz, 2H), 3.77 (d, *J*=6.0Hz, 2H), 2.10 (t, *J*=7.5Hz, 2H), 2.00-1.95 (m, 4H), 1.52 (*p*,

*J*=7.0Hz, 2H), 1.28-1.23 (m, 16H), 1.17 (t, *J*=7.0Hz, 3H), 0.84 (t, *J*=7.0Hz, 3H) . $^{13}$C NMR (100 MHz, DMSO-$d_6$): δ 172.73, 170.19, 130.34, 129.22, 60.45, 40.80, 34.70, 31.47, 29.32, 29.22, 29.10, 29.08, 28.88, 28.83, 26.79, 2636, 25.51, 22.27, 14.24, 14.13. HRMS (ESI) *m/z* $[M+H]^+$ calcd for $C_{20}H_{38}NO_3$, 340.2846; found, 340.2849.

**ethyl 2-[[(Z)-hexadec-4-enoyl]amino]acetate.** Yield = 56%, colourless liquid. $^1$H NMR (500 MHz, DMSO-$d_6$) δ 8.23 (t, *J*=6.0Hz, 1H), 5.32–5.30 (m, 2H), 4.06 (q, *J*=7.0Hz, 2H), 3.77 (d, *J*=6.0Hz, 2H), 2.20 (t, *J*=7.0Hz, 2H), 2.15-2.12 (m, 2H), 1.99-1.97 (m, 2H), 1.29-1.23(m, 16H), 1.17 (t, *J*=7.0Hz, 3H), 0.84 (t, *J*=7.0Hz, 3H) . $^{13}$C NMR (100 MHz, DMSO-$d_6$): δ 172.08, 169.93, 130.21, 129.36, 60.29, 40.60, 34.98, 31.28, 29.04, 29.02, 28.99, 28.91, 28.70, 26.64, 26.57, 23.01, 22.08, 20.74, 14.04, 13.93. HRMS (ESI) *m/z* $[M+H]^+$ calcd for $C_{20}H_{38}NO_3$, 340.2846; found, 340.2848.

**ethyl 2-[[(Z)-tetradec-9-enoyl]amino]acetate.** Yield = 70%, colourless liquid. $^1$H NMR (500 MHz, DMSO-$d_6$): δ 8.19 (t, *J*=6.0Hz, 1H), 5.32–5.30 (m, 2H), 4.07 (q, *J*=7.0Hz, 2H), 3.77 (d, *J*=6.0Hz, 2H), 2.10 (t, *J*=7.5Hz, 2H), 2.05-1.90 (m, 4H), 1.47 (p, *J*=7.5Hz, 2H), 1.30-1.20 (m, 12H), 1.17 (t, *J*=7.0Hz, 2H), 0.85 (t, *J*=7.0Hz, 3H) . $^{13}$C NMR (100 MHz, DMSO-$d_6$): δ 172.64, 169.97, 129.61, 129.58, 60.26, 40.60, 34.97, 31.35, 29.09, 28.65, 28.52, 28.51, 26.58, 26.30, 25.15, 21.69, 14.04, 13.79. HRMS (ESI) *m/z* $[M+H]^+$ calcd for $C_{18}H_{34}NO_3$, 312.2533; found, 312.2529.

**General procedure for synthesis of 3 – 20**

To a solution of the ethyl ester (0.51 mmol) in ethanol (30 mL), was added 1M NaOH (10 mL). The solution was stirred at 40 $^{o}$C for 3 h. The ethanol was removed under reduced pressure, and the aqueous residue was adjusted to pH 2 with 0.5 M HCl. The resulting suspension was filtered and the solid product washed with water (10 mL) and ethanol (5 mL).

**2-[[(Z)-octadec-15-enoyl]amino]acetic acid (3).** Yield = 87%, white powder. Mp. = 87 - 89 $^{o}$C. $^{1}$H NMR (500 MHz, $CDCl_3$) δ 6.02 (s, 1H), 5.40–5.30 (m, 2H), 4.09 (d, *J*=5.5Hz, 2H), 2.27 (t, *J*=7.5Hz, 2H), 2.10-1.95 (m, 4H), 1.65 (p, *J*=7.0Hz, 2H), 1.35-1.20 (m, 20H), 0.96 (t, *J*=7.5Hz, 3H). $^{13}$C NMR (100 MHz, DMSO-$d_6$): δ 172.95, 171.86, 131.71, 129.46, 40.97, 35.50, 29.56, 29.46, 29.44, 29.38, 29.32, 29.25, 29.05, 29.04, 26.93, 25.63, 20.46, 14.69. HRMS (ESI) *m/z* $[M+H]^+$ calcd for $C_{20}H_{38}NO_3$, 340.2846; found, 340.2847. Anal. Calcd for $C_{20}H_{37}NO_3.1/4H_2O$: C 69.83, H 10.99, N 4.07. Found: C 69.95, H 11.17, N 4.03.

**2-[[(Z)-octadec-13-enoyl]amino]acetic acid (4).** Yield = 77%, white powder. Mp. = 95 - 96 $^{o}$C. $^{1}$H NMR (500 MHz, DMSO-$d_6$): δ 8.06 (t, *J*=5.5Hz, 1H), 5.32–5.30 (m, 2H), 3.70 (d, *J*=6.0HZ, 2H), 2.09 (t, *J*=7.5Hz, 2H), 1.98-1.95 (m, 4H), 1.47 (*p*, *J*=7.0Hz, 2H), 1.31-1.23 (m, 20H), 0.84 (t, *J*=7.0Hz, 3H). $^{13}$C NMR (100 MHz, DMSO-$d_6$): δ 172.37, 171.38, 129.63, 129.59, 40.82, 35.09, 31.36, 29.08, 29.00 (2C), 28.94, 28.85, 28.81, 28.62, 28.57, 26.55, 26.30, 25.19, 21.70, 13.81. HRMS (ESI) *m/z* $[M+H]^+$ calcd for $C_{20}H_{38}NO_3$, 340.2846; found, 340.2850. Anal. Calcd for $C_{20}H_{37}NO_3.1/4H_2O$: C 69.83, H 10.99, N 4.07. Found: C 69.88, H 11.03, N 4.15.

**2-[[(Z)-octadec-12-enoyl]amino]acetic acid (5).** Yield = 78%, white powder. Mp. = 94 - 95 $^{o}$C. $^{1}$H NMR (500 MHz, DMSO-$d_6$): δ 7.90 (t, *J*=5.5Hz, 1H), 5.32–5.30 (m, 2H), 3.61(d, *J*=5.5HZ, 2H), 2.08(t, *J*=7.5Hz, 2H), 1.99-1.95(m, 4H), 1.46 (*p*, *J*=7.0Hz, 2H), 1.30-1.22 (m, 20H), 0.84 (t, *J*=7.0Hz, 3H) . $^{13}$C NMR (100 MHz, DMSO-$d_6$): δ. 172.33, 171.35, 129.62, 129.61, 40.84, 35.08, 30.85, 29.07, 28.92, 28.84 (2C), 28.80, 28.79 (2C), 28.61, 28.56, 26.54, 25.18, 21.95, 13.91. HRMS (ESI) *m/z* $[M+H]^+$ calcd for $C_{20}H_{38}NO_3$, 340.2846; found, 340.2850. Anal. Calcd for $C_{20}H_{37}NO_3.1/2H_2O$: C 68.92, H 10.99, N 3.92. Found: C 68.61, H 11.03, N 3.96.

**2-[[(Z)-octadec-11-enoyl]amino]acetic acid (6).** Yield = 87%, white powder. Mp. = 92 - 93 $^{o}$C. $^{1}$H NMR (500 MHz, DMSO-$d_6$): δ 8.00 (t, *J*=5.5Hz, 1H), 5.32–5.30 (m, 2H), 3.65 (d, *J*=6.0Hz, 2H), 2.07 (t, *J*=7.5Hz, 2H), 1.99-1.95(m, 4H), 1.46 (*p*, *J*=6.5Hz, 2H), 1.30-1.22(m, 20H), 0.84 (t, *J*=7.0Hz, 3H). $^{13}$C NMR (100 MHz, DMSO-$d_6$): δ 172.53, 171.61, 129.80 (2C), 41.03, 40.20, 35.27, 31.30, 29.28, 29.26, 29.11, 29.04, 28.99, 28.81, 28.77, 28.44, 26.76, 25.37, 22.26, 14.10. HRMS (ESI) *m/z* $[M+H]^+$ calcd for $C_{20}H_{38}NO_3$, 340.2846; found, 340.2840. Anal. Calcd for $C_{20}H_{37}NO_3.1/4H_2O$: C 69.83, H 10.99, N 4.07. Found: C 69.84, H 11.01, N 3.94.

**2-[[(Z)-octadec-10-enoyl]amino]acetic acid (7).** Yield = 92%, white powder. Mp. = 85 - 86 $^{o}$C. $^{1}$H NMR (500 MHz, DMSO-$d_6$): δ 8.04 (t, *J*=5.5Hz, 1H), 5.32–5.30 (m, 2H), 3.70 (d, *J*=6.0HZ, 2H), 2.08 (t, *J*=7.5Hz, 2H), 1.99-1.95 (m, 4H), 1.47 (*p*, *J*=7.0Hz, 2H), 1.30-1.23 (m, 20H), 0.84 (t, *J*=7.0Hz, 3H). $^{13}$C NMR (100 MHz, DMSO-$d_6$): δ 172.06, 171.00, 129.25, 129.24, 40.96, 34.67, 30.87, 28.72, 28.70, 28.40, 28.20 (2C), 28.14 (2C), 28.12 26.20 26.16, 24.78, 21.67, 13.55. HRMS (ESI) *m/z* $[M+H]^+$ calcd for $C_{20}H_{38}NO_3$, 340.2846; found, 340.2851. Anal. Calcd for $C_{20}H_{37}NO_3.1/2H_2O$: C 68.92, H 10.99, N 3.92. Found: C 68.90, H 10.64, N 3.94.

**2-[[(Z)-octadec-8-enoyl]amino]acetic acid (8).** Yield = 96%, white powder. Mp. = 91 - 92 $^{o}$C. $^{1}$H NMR (500 MHz, DMSO-$d_6$): δ 8.02 (t, *J*=5.0Hz, 1H), 5.32–5.30 (m, 2H), 3.70 (d, *J*=6.0HZ, 2H), 2.09(t, *J*=7.5Hz, 2H), 1.98-1.95 (m, 4H), 1.46 (*p*, *J*=7.0Hz, 2H), 1.31-1.23 (m, 20H), 0.84 (t, *J*=7.0Hz, 3H). $^{13}$C NMR (100 MHz, DMSO-$d_6$): δ 172.44, 171.44, 129.64, 129.62, 40.68, 35.06, 31.28, 29.10, 29.07, 28.98, 28.87, 28.68, 28.58, 28.50, 28.44, 26.61, 26.57, 25.17, 22.09, 13.95. HRMS (ESI) *m/z* $[M+H]^+$ calcd for $C_{20}H_{38}NO_3$, 340.2846; found, 340.2847. Anal. Calcd for $C_{20}H_{37}NO_3.1/2H_2O$: C 68.92, H 10.99, N 3.92. Found: C 68.84, H 11.02, N 3.97.

**2-[[(Z)-octadec-7-enoyl]amino]acetic acid (9).** Yield = 92%, white powder. Mp. = 86 - 87 $^{o}$C. $^{1}$H NMR (500 MHz, DMSO-$d_6$): δ 8.10 (t, *J*=5.5Hz, 1H), 5.32–5.30 (m, 2H), 3.70 (d, *J*=6.0HZ, 2H), 2.10 (t, *J*=7.0Hz, 2H), 1.97 (m, 4H), 1.48 (*p*, *J*=7.0Hz, 2H), 1.31-1.23 (m, 20H), 0.84 (t, *J*=7.0Hz, 3H). $^{13}$C NMR (100 MHz, DMSO-$d_6$): δ 172.63, 171.60, 129.84, 129.75, 40.75, 35.20, 31.47, 29.28, 29.19, 29.16, 29.13, 29.05, 28.87, 28.77, 28.45, 26.76, 26.74, 25.25, 22.27, 14.13. HRMS (ESI) *m/z* $[M+H]^+$ calcd for $C_{20}H_{38}NO_3$, 340.2846; found, 340.2851. Anal. Calcd for $C_{20}H_{37}NO_3$: C 70.75, H 10.98, N 4.13. Found: C 70.75, H 11.16, N 4.18.

**2-[[(Z)-octadec-6-enoyl]amino]acetic acid (10).** Yield = 89%, white powder. Mp. = 90 - 91 $^{o}$C. $^{1}$H NMR (500 MHz, DMSO-$d_6$): δ 8.04 (t, *J*=5.5Hz, 1H), 5.32–5.30 (m, 2H), 3.70 (d, *J*=6.0Hz, 2H), 2.10 (t, *J*=7.0Hz, 2H), 1.98-1.95 (m, 4H), 1.48 (*p*, *J*=7.5Hz, 2H), 1.30-1.23 (m, 20H), 0.84 (t, *J*=7.0Hz, 3H). $^{13}$C NMR (100 MHz, DMSO-$d_6$): δ 172.34, 171.38, 129.75, 129.43, 40.67, 34.91, 31.28, 29.11, 29.02, 28.99, 28.98, 28.87, 28.70, 28.69, 28.61, 26.59, 26.44, 24.83, 22.08, 13.95. HRMS (ESI) *m/z* $[M+H]^+$ calcd for $C_{20}H_{38}NO_3$, 340.2846; found, 340.2845. Anal. Calcd for $C_{20}H_{37}NO_3$: C 70.75, H 10.98, N 4.13. Found: C 70.56, H 11.28, N 4.01.

**2-[[(E)-octadec-11-enoyl]amino]acetic acid (11).** Yield = 82%, white powder. Mp. = 98 - 99 $^{o}$C. $^{1}$H NMR (500 MHz, DMSO-$d_6$): δ 7.94 (t, *J*=5.5Hz, 1H), 5.36–5.34 (m, 2H), 3.65 (d, *J*=6.0Hz, 2H), 2.08 (t, *J*=7.0Hz, 2H), 1.93-1.92 (m, 4H), 1.46 (*p*, *J*=6.5Hz, 2H), 1.28-1.22(m, 20H), 0.84 (t, *J*=7.0Hz, 3H). $^{13}$C NMR (100 MHz, DMSO-$d_6$): δ 172.57, 171.55, 130.25, 40.96, 35.27, 32.11, 31.27, 29.17, 29.14 (2C), 29.11, 29.01, 28.96 (2C), 28.79, 28.64, 28.30, 25.36, 22.25, 14.11. HRMS (ESI) *m/z* $[M+H]^+$ calcd for $C_{20}H_{38}NO_3$, 340.2846; found, 340.2852. Anal. Calcd for $C_{20}H_{37}NO_3.1/4H_2O$: C 69.83, H 10.99, N 4.07. Found: C 69.84, H 11.01, N 3.94.

**2-[[(E)-octadec-9-enoyl]amino]acetic acid (12).** Yield = 93%, white powder. Mp. = 105 - 106 $^{o}$C. $^{1}$H NMR (500 MHz, DMSO-$d_6$): δ 8.04(t, *J*=5.5Hz, 1H), 5.36–5.40 (m, 2H), 3.70 (d, *J*=6.0Hz, 2H), 2.10 (t, *J*=7.0Hz, 2H), 1.94-1.91 (m, 4H), 1.48 (*p*, *J*=7.0Hz, 2H), 1.30-1.23 (m, 20H), 0.84 (t, *J*=7.0Hz, 3H). $^{13}$C NMR (100 MHz, DMSO-$d_6$): δ 172.67, 171.60, 130.24, 40.73, 40.20, 35.22, 32.11, 31.44, 29.17, 28.99 (4C), 28.86, 28.77, 28.65, 28.59, 25.34, 22.25, 14.12. HRMS (ESI) *m/z* $[M+H]^+$ calcd for $C_{20}H_{38}NO_3$, 340.2846; found, 340.2851. Anal. Calcd for $C_{20}H_{37}NO_3$: C 70.75, H 10.98, N 4.13. Found: C 70.42, H 11.24, N 4.00.

**2-[[(Z)-hexadec-13-enoyl]amino]acetic acid (13).** Yield = 88%, white powder. Mp. = 84 - 86 $^{o}$C. $^{1}$H NMR (500 MHz, DMSO-$d_6$) δ 8.06 (t, *J*=5.5Hz, 1H), 5.35–5.25 (m, 2H), 3.76 (d, *J*-5.5Hz, 2H), 2.08 (t, *J*=7.5Hz, 2H), 2.00-1.90 (m, 4H), 1.46 (p, *J*=7.0Hz, 2H), 1.30-1.10 (m, 16H), 0.88 (t, *J*=7.0Hz, 3H). $^{13}$C NMR (100 MHz, DMSO-$d_6$): δ 172.95, 171.86, 131.71, 129.46, 40.97, 35.50, 29.56, 29.46, 29.44, 29.38, 29.32, 29.25, 29.05, 29.04, 26.93, 25.63, 20.46, 14.69. HRMS (ESI) *m/z* $[M+H]^+$ calcd for $C_{18}H_{43}NO_3$, 312.2533; found, 312.2529. Anal. Calcd for $C_{18}H_{33}NO_3$: C 69.41, H 10.68, N 4.50. Found: C 69.33, H 10.71, N 4.34.

**2-[[(Z)-hexadec-11-enoyl]amino]acetic acid (14).** Yield = 65%, white powder. Mp. = 85 - 86 ºC. $^{1}$H NMR (500 MHz, DMSO-$d_6$): δ 8.07 (t, *J*=5.5Hz, 1H), 5.32–5.30 (m, 2H), 3.70 (d, *J*=5.5Hz, 2H), 2.09 (t, *J*=7.5Hz, 2H), 1.98-1.95 (m, 4H), 1.46 (*p*, *J*=7.0Hz, 2H), 1.31-1.23(m, 16H), 0.84 (t, *J*=7.0Hz, 3H). $^{13}$C NMR (100 MHz, DMSO-$d_6$): δ 172.56, 171.44, 129.65, 129.61, 40.60, 35.06, 31.37, 29.11, 28.93, 28.84 (2C), 28.800, 28.61, 28.59, 26.58, 26.31, 25.10, 21.71, 13.82. HRMS (ESI) *m/z* $[M+H]^+$ calcd for $C_{18}H_{34}NO_3$, 312.2533; found, 312.2534. Anal. Calcd for $C_{18}H_{33}NO_3$: C 69.41, H 10.68, N 4.50. Found: C 69.57, H 10.87, N 4.32.

**2-[[(Z)-hexadec-10-enoyl]amino]acetic acid (15).** Yield = 72%, white powder. Mp. = 82 - 83 ºC. $^{1}$H NMR (500 MHz, DMSO-$d_6$): δ 8.02 (t, *J*=5.5Hz, 1H), 5.32–5.30 (m, 2H), 3.68(d, *J*=6.0Hz, 2H), 2.08 (t, *J*=7.5Hz, 2H), 1.99-1.95 (m, 4H), 1.46 (*p*, *J*=7.0Hz, 2H), 1.30-1.22 (m, 16H), 0.84 (t, *J*=7.0Hz, 3H). $^{13}$C NMR (100 MHz, DMSO-$d_6$): δ 172.64, 171.58, 129.83 (2C), 40.83, 35.25, 31.04, 29.29, 28.98 (2C), 28.78 (2C), 28.76, 26.77, 26.74, 25.17, 22.15, 14.11. HRMS (ESI) *m/z* $[M+H]^+$ calcd for $C_{18}H_{34}NO_3$, 312.2533; found, 312.2535. Anal. Calcd for $C_{18}H_{33}NO_3$: C 69.41, H 10.68, N 4.50. Found: C 69.45, H 10.92, N 4.35.

**2-[[(Z)-hexadec-9-enoyl]amino]acetic acid (16).** Yield = 92%, white powder. Mp. = 83 - 84 ºC. $^{1}$H NMR (500 MHz, DMSO-$d_6$): δ 8.05 (t, *J*=5.5Hz, 1H), 5.32–5.30 (m, 2H), 3.68 (d, *J*=6.0HZ, 2H), 2.09 (t, *J*=7.5Hz, 2H), 1.98-1.96(m, 4H), 1.46 (*p*, *J*=6.5Hz, 2H), 1.28-1.23 (m, 16H), 0.84 (t, *J*=7.0Hz, 3H). $^{13}$C NMR (100 MHz, DMSO-$d_6$): δ 172.49, 171.41, 129.63 (2C), 40.56, 35.04, 31.11, 29.08, 29.07, 28.67, 28.58, 28.52 (2C), 28.25, 26.58, 25.16, 22.07, 13.93. HRMS (ESI) *m/z* $[M+H]^+$ calcd for $C_{18}H_{34}NO_3$, 312.2533; found, 312.2532. Anal. Calcd for $C_{18}H_{33}NO_3.1/4H_2O$: C 68.42, H 10.69, N 4.43. Found: C 68.71, H 10.79, N 4.45.

**2-[[(Z)-hexadec-7-enoyl]amino]acetic acid (17).** Yield = 78%, white powder. Mp. = 82 - 83 $^{o}$C. $^{1}$H NMR (500 MHz, DMSO-$d_6$): δ 8.02 (t, *J*=5.5Hz, 1H), 5.32–5.30 (m, 2H), 3.67 (d, *J*=5.5Hz, 2H), 2.09 (t, *J*=7.5Hz, 2H), 1.97-1.96 (m, 4H), 1.47 (*p*, *J*=7.0Hz, 2H), 1.30-1.23 (m, 16H), 0.84 (t, *J*=7.0Hz, 3H). $^{13}$C NMR (100 MHz, DMSO-$d_6$): δ 172.44, 171.42, 129.65, 129.58, 40.60, 35.02, 31.27, 29.11, 28.95, 28.84, 28.67, 28.61, 28.27, 26.58, 26.56, 25.07, 22.08, 13.95. HRMS (ESI) *m/z* $[M+H]^+$ calcd for $C_{18}H_{34}NO_3$, 312.2533; found, 312.2535. Anal. Calcd for $C_{18}H_{33}NO_3$: C 69.41, H 10.68, N 4.50. Found: C 69.72, H 10.98, N 4.47.

**2-[[(Z)-hexadec-5-enoyl]amino]acetic acid (18).** Yield = 66%, white powder. Mp. = 88 - 89 $^{o}$C. $^{1}$H NMR (500 MHz, DMSO-$d_6$): δ 8.00 (t, *J*=5.5Hz, 1H), 5.32–5.30 (m, 2H), 3.60 (d, *J*=5.5Hz, 2H), 2.10(t, *J*=7.5Hz, 2H), 1.97-1.95 (m, 4H), 1.51 (*p, J*=7.5Hz, 2H), 1.28-1.23(m, 16H), 0.84 (t, *J*=7.0Hz, 3H). $^{13}$C NMR (100 MHz, DMSO-$d_6$): δ 172.63, 171.62, 129.84, 129.77, 40.79, 35.22, 31.47, 29.30, 29.14, 29.03 (2C), 28.87, 28.79, 28.46, 26.75, 25.26, 22.28, 14.14. HRMS (ESI) *m/z* $[M+H]^+$ calcd for $C_{18}H_{34}NO_3$, 312.2533; found, 312.2536. Anal. Calcd for $C_{18}H_{33}NO_3$: C 69.41, H 10.68, N 4.50. Found: C 69.46, H 10.83, N 4.53.

**2-[[(Z)-hexadec-4-enoyl]amino]acetic acid (19).** Yield = 60%, white powder. Mp. = 116 - 117 $^{o}$C. $^{1}$H NMR (500 MHz, DMSO-$d_6$): δ 7.70 (t, *J*=5.5Hz, 1H), 5.32–5.30 (m, 2H), 3.51 (d, *J*=5.0Hz, 2H), 2.20 (m, 2H), 2.10 (t, *J*=6.5Hz,2H), 1.98-1.95 (m, 2H), 1.40-1.23 (m, 18H), 0.84 (t, *J*=7.0Hz, 3H). $^{13}$C NMR (100 MHz, DMSO-$d_6$): δ 172.65, 171.63, 129.82, 129.79, 40.68, 35.10, 31.42, 29.34, 29.24, 29.07 (2C), 28.86, 28.77, 28.48, 26.72, 25.23, 22.27, 14.14. HRMS (ESI) *m/z* $[M+H]^+$ calcd for $C_{18}H_{34}NO_3$, 312.2533; found, 312.2535. Anal. Calcd for $C_{18}H_{33}NO_3.H_2O$: C 65.62, H 10.71, N 4.25. Found: C 65.77, H 10.36, N 4.23.

**2-[[(Z)-tetradec-9-enoyl]amino]acetic acid (20).** Yield = 93%, white powder. Mp. = 70 - 71 $^{o}$C. $^{1}$H NMR (500 MHz, DMSO-$d_6$): δ 8.09 (t, *J*=6.0Hz, 1H), 5.32–5.30 (m, 2H), 3.69 (d, *J*=6.0Hz, 2H), 2.09 (t, *J*=7.5Hz, 2H), 2.05-1.90 (m, 4H), 1.45 (p, *J*=7.5Hz,2H), 1.30-1.18 (m, 12H), 0.84 (t, *J*=7.0Hz, 3H). $^{13}$C NMR (100 MHz, DMSO-$d_6$): δ 172.58, 171.44, 129.66, 129.62, 40.57, 35.8, 31.37, 29.11, 28.68, 28.60, 28.54, 26.60, 26.32, 25.20, 21.72, 13.84. HRMS (ESI) *m/z* $[M+H]^+$ calcd for $C_{16}H_{30}NO_3$, 284.2202; found, 284.2208. Anal. Calcd for $C_{16}H_{29}NO_3.3/4H_2O$: C 64.72, H 10.35, N 4.72. Found: C 65.08, H 9.98, N 4.78.

**Oocyte harvesting and glycine transporter expression**

GlyT2a and GlyT1b cDNA were subcloned into pOTV (plasmid oocyte transcription vector), plasmids were linearised using *Spe*I (New England Biolabs (Genesearch) Arundel, Australia), and mRNA was transcribed using T7 RNA polymerase (mMessagemMachine kit, Ambion, TX, USA). Oocytes were surgically removed from *Xenopus laevis* frogs as previously described[41] in accordance with the Australian Code of Practice for the Care and Use of Animals for Scientific Purposes. Defoliculated stage V-VI oocytes were injected with mRNA (Drummond Nanoinject, Drummond Scientific Co., Broomall, PA, USA), and stored in standard frog Ringer's solution (ND96), supplemented with 2.5 mM sodium pyruvate, 0.5 mM theophylline, 50 µg/mL gentamicin and 100 µM/mL tetracycline until transporter expression levels were sufficient to measure transporter function.

**Electrophysiology**

2-5 days following injection, glycine transport currents were measured at -60 mV using Geneclamp 500 amplifier (Axon Instruments, Foster City, CA, USA) with a Powerlab 2/20 chart recorder (ADInstruments, Sydney, Australia) using chart software

(ADInstruments). Synthesised acyl-glycines were dissolved in DMSO (10 mg/mL) and co-applied with the $EC_{50}$ concentration of glycine to the recording bath until transport current was reduced. ND96 was then perfused over the oocyte for five minutes to wash the bath and restore glycine transport.

**$^{3}$H-Glycine Uptake assays**

Oocytes expressing GlyT2 as well as uninjected controls were pre-incubated with 3 µM acyl-glycine lipids for 2 minutes at room temperature and then incubated with 10 µM $^{3}$H-Glycine for 0.5, 1, 2, 5 and 10 minutes and then washed 3 times in ice cold ND96. Oocytes were then placed in 0.1 M NaOH for 30 minutes to lyse the oocytes. Scintillant was added and the $^{3}$H counted in a Trilux beta counter. The rate of uptake was estimated by fitting the linear portion of the time course to a straight line.

**Data analysis**

Data analysis was performed in GraphPad Prism 7.02 (GraphPad Software, San Diego, CA, USA). $IC_{50}$ values were calculated using least-squares curve fitting analysis and presented as mean ± SEM. Inhibition-concentration curves were generated using the equation: $Y = Bottom + (Top-Bottom)/(1+10^{[I]-logIC50})$, where [I] is log[acyl-glycine] (µM), Y is current normalised to glycine without inhibitor present, and Top and Bottom are the maximal and minimal plateau responses respectively. This equation was constrained to have the bottom value > 0 and the standard hill slope -1.0. .

**Materials**

All chemicals were obtained from Sigma Chemical Co. (Sydney, Australia) unless otherwise stated.

## Abbreviations

GlyT: Glycine Transporter, NAGly: N-arachidonyl-glycine, OLCarn: Oleoyl-L-carnitine, CMC: Critical Micelle Concentration, CB: Cannabinoid

## Author Information

Current Address for Jane Carland is St Vincents Hospital, Darlinghurst, NSW 2010, Australia

## Author Contributions.

SM conducted and designed experiments, analysed data, wrote the manuscript. JC conducted and designed experiments, analysed data. SS conducted experiments and analysed data. RR, TR and RV designed experiments, analysed data and wrote the manuscript.

## Funding Sources

This work was supported by a NHMRC Project Grant APP1082570 (RR, TR, RR). SM is supported by an Australian Postgraduate Award.

## Conflict of Interest

There are no conflicts of interest to be declared

## Acknowledgments

We thank Chery Handford for her expert assistance in maintaining the *Xenopus laevis* facility

## REFERENCES


1. Landreh, M., Marty, M. T., Gault, J., and Robinson, C. V. (2016) A sliding selectivity scale for lipid binding to membrane proteins, *Curr Opin Struct Biol 39*, 54-60.
2. Koshy, C., Schweikhard, E. S., Gartner, R. M., Perez, C., Yildiz, O., and Ziegler, C. (2013) Structural evidence for functional lipid interactions in the betaine transporter BetP, *EMBO J 32*, 3096-3105.
3. Bai, J. Y., Ding, W. G., Kojima, A., Seto, T., and Matsuura, H. (2015) Putative binding sites for arachidonic acid on the human cardiac Kv 1.5 channel, *Br J Pharmacol 172*, 5281-5292.
4. Chrencik, J. E., Roth, C. B., Terakado, M., Kurata, H., Omi, R., Kihara, Y., Warshaviak, D., Nakade, S., Asmar-Rovira, G., Mileni, M., Mizuno, H., Griffith, M. T., Rodgers, C., Han, G. W., Velasquez, J., Chun, J., Stevens, R. C., and Hanson, M. A. (2015) Crystal Structure of Antagonist Bound Human Lysophosphatidic Acid Receptor 1, *Cell 161*, 1633-1643.
5. Hite, R. K., Butterwick, J. A., and MacKinnon, R. (2014) Phosphatidic acid modulation of Kv channel voltage sensor function, *Elife 3*.
6. Hurst, D. P., Grossfield, A., Lynch, D. L., Feller, S., Romo, T. D., Gawrisch, K., Pitman, M. C., and Reggio, P. H. (2010) A lipid pathway for ligand binding is necessary for a cannabinoid G protein-coupled receptor, *J Biol Chem 285*, 17954-17964.
7. Pei, Y., Mercier, R. W., Anday, J. K., Thakur, G. A., Zvonok, A. M., Hurst, D., Reggio, P. H., Janero, D. R., and Makriyannis, A. (2008) Ligand-binding architecture of human CB2 cannabinoid receptor: evidence for receptor subtype-specific binding motif and modeling GPCR activation, *Chem Biol 15*, 1207-1219.
8. Bradshaw, H. B., Rimmerman, N., Hu, S. S., Benton, V. M., Stuart, J. M., Masuda, K., Cravatt, B. F., O'Dell, D. K., and Walker, J. M. (2009) The endocannabinoid anandamide is a precursor for the signaling lipid N-arachidonoyl glycine by two distinct pathways, *BMC Biochem 10*, 14.
9. Huang, S. M., Bisogno, T., Petros, T. J., Chang, S. Y., Zavitsanos, P. A., Zipkin, R. E., Sivakumar, R., Coop, A., Maeda, D. Y., De Petrocellis, L., Burstein, S., Di Marzo, V., and Walker, J. M. (2001) Identification of a new class of molecules, the arachidonyl amino acids, and characterization of one member that inhibits pain, *J Biol Chem 276*, 42639-42644.
10. Succar, R., Mitchell, V. A., and Vaughan, C. W. (2007) Actions of N-arachidonyl-glycine in a rat inflammatory pain model, *Mol Pain 3*, 24.
11. Vuong, L. A., Mitchell, V. A., and Vaughan, C. W. (2008) Actions of N-arachidonyl-glycine in a rat neuropathic pain model, *Neuropharmacology 54*, 189-193.
12. Sheskin T., H. L., Slager J., Vogel Z., and Mechoulam R. (1997) Structural requirements for binding of anandamide-type compounds to the brain cannabinoid receptor, *J Med Chem 40*, 659-667.
13. Jeong, H. J., Vandenberg, R. J., and Vaughan, C. W. (2010) N-arachidonyl-glycine modulates synaptic transmission in superficial dorsal horn, *Br J Pharmacol 161*, 925-935.
14. Wiles, A. L., Pearlman, R. J., Rosvall, M., Aubrey, K. R., and Vandenberg, R. J. (2006) N-Arachidonyl-glycine inhibits the glycine transporter, GLYT2a, *J Neurochem 99*, 781-786.
15. Zeilhofer, H. U., Studler, B., Arabadzisz, D., Schweizer, C., Ahmadi, S., Layh, B., Bosl, M. R., and Fritschy, J. M. (2005) Glycinergic neurons expressing

enhanced green fluorescent protein in bacterial artificial chromosome transgenic mice, *J Comp Neurol 482*, 123-141.
16. Imlach, W. L., Bhola, R. F., Mohammadi, S. A., and Christie, M. J. (2016) Glycinergic dysfunction in a subpopulation of dorsal horn interneurons in a rat model of neuropathic pain, *Sci Rep 6*, 37104.
17. Roux, M. J., and Supplisson, S. (2000) Neuronal and glial glycine transporters have different stoichiometries, *Neuron 25*, 373-383.
18. Zafra, F., Aragon, C., Olivares, L., Danbolt, N. C., Gimenez, C., and Storm-Mathisen, J. (1995) Glycine transporters are differentially expressed among CNS cells, *J Neurosci 15*, 3952-3969.
19. Gomeza, J. , Ohno, K., Hu, S., Wencke Armsen, I. Eulenburg, V., Richter, D.W., Laube, B., and Betz, H. (2003)Deletion of the Mouse Glycine Transporter 2 Results in a Hyperekplexia Phenotype and Postnatal Lethality *Neuron*, Vol. 40, 797–806.
20. Vandenberg, R. J., Mostyn, S. N., Carland, J. E., and Ryan, R. M. (2016) Glycine transporter2 inhibitors: Getting the balance right, *Neurochem Int 98*, 89-93.
21. Mingorance-Le Meur, A., Ghisdal, P., Mullier, B., De Ron, P., Downey, P., Van Der Perren, C., Declercq, V., Cornelis, S., Famelart, M., Van Asperen, J., Jnoff, E., and Courade, J. P. (2013) Reversible inhibition of the glycine transporter GlyT2 circumvents acute toxicity while preserving efficacy in the treatment of pain, *Br J Pharmacol 170*, 1053-1063.
22. Morita, K., Motoyama, N., Kitayama, T., Morioka, N., Kifune, K., and Dohi, T. (2008) Spinal antiallodynia action of glycine transporter inhibitors in neuropathic pain models in mice, *J Pharmacol Exp Ther 326*, 633-645.
23. Prusakiewicz, J. J., Kingsley, P. J., Kozak, K. R., and Marnett, L. J. (2002) Selective oxygenation of N-arachidonylglycine by cyclooxygenase-2, *Biochem Biophys Res Commun 296*, 612-617.
24. Carland, J. E., Mansfield, R. E., Ryan, R. M., and Vandenberg, R. J. (2013) Oleoyl-L-carnitine inhibits glycine transport by GlyT2, *Br J Pharmacol 168*, 891-902.
25. Arduini, A., Mancinelli, G., Radatti, G. L., Dottori, S., Molajoni, F., and Ramsay, R. R. (1992) Role of carnitine and carnitine palmitoyltransferase as integral components of the pathway for membrane phospholipid fatty acid turnover in intact human erythrocytes, *J Biol Chem 267*, 12673-12681.
26. Thomas, B. F., Adams, I. B., Mascarella, S. W., Martin, B. R., and Razdan, R. K. (1996) Structure-activity analysis of anandamide analogs: relationship to a cannabinoid pharmacophore, *J Med Chem 39*, 471-479.
27. Lin, S., Khanolkar, A. D., Fan, P., Goutopoulos, A., Qin, C., Papahadjis, D., and Makriyannis, A. (1998) Novel analogues of arachidonylethanolamide (anandamide): affinities for the CB1 and CB2 cannabinoid receptors and metabolic stability, *J Med Chem 41*, 5353-5361.
28. Rawling, T., Duke, C. C., Cui, P. H., and Murray, M. (2010) Facile and stereoselective synthesis of (Z)-15-octadecenoic acid and (Z)-16-nonadecenoic acid: monounsaturated omega-3 fatty acids, *Lipids 45*, 159-165.
29. Baur, B., Gertsch, J. and Sigel, E. (2013) Do N-arachidonyl-glycine (NA-glycine) and 2-arachidonoyl glycerol (2-AG) share mode of action and the binding site on the β2 subunit of $GABA_A$ receptors? *PeerJ* 1:e149
30. Vandenberg, R. J., Shaddick, K., and Ju, P. (2007) Molecular basis for substrate discrimination by glycine transporters, *J Biol Chem 282*, 14447-14453.
31. Edington, A. R., McKinzie, A. A., Reynolds, A. J., Kassiou, M., Ryan, R. M., and Vandenberg, R. J. (2009) Extracellular loops 2 and 4 of GLYT2 are required for

N-arachidonylglycine inhibition of glycine transport, *J Biol Chem 284*, 36424-36430.
32. Funari, S. S., Barcelo, F., and Escriba, P. V. (2003) Effects of oleic acid and its congeners, elaidic and stearic acids, on the structural properties of phosphatidylethanolamine membranes, *J Lipid Res 44*, 567-575.
33. van Meer, G., Voelker, D. R., and Feigenson, G. W. (2008) Membrane lipids: where they are and how they behave, *Nat Rev Mol Cell Biol 9*, 112-124.
34. Hua, T., Vemuri, K., Pu, M., Qu, L., Han, G. W., Wu, Y., Zhao, S., Shui, W., Li, S., Korde, A., Laprairie, R. B., Stahl, E. L., Ho, J. H., Zvonok, N., Zhou, H., Kufareva, I., Wu, B., Zhao, Q., Hanson, M. A., Bohn, L. M., Makriyannis, A., Stevens, R. C., and Liu, Z. J. (2016) Crystal Structure of the Human Cannabinoid Receptor CB1, *Cell 167*, 750-762 e714.
35. Stanley, N., Pardo, L., and Fabritiis, G. D. (2016) The pathway of ligand entry from the membrane bilayer to a lipid G protein-coupled receptor, *Sci Rep 6*, 22639.
36. Liin, S. I., Larsson, J. E., Barro-Soria, R., Bentzen, B. H., and Larsson, H. P. (2016) Fatty acid analogue N-arachidonoyl taurine restores function of IKs channels with diverse long QT mutations, *Elife 5*.
37. Berglund, B. A., Boring, D. L., Wilken, G. H., Makriyannis, A., Howlett, A. C., and Lin, S. (1998) Structural requirements for arachidonylethanolamide interaction with CB1 and CB2 cannabinoid receptors: pharmacology of the carbonyl and ethanolamide groups, *Prostaglandins Leukot Essent Fatty Acids 59*, 111-118.
38. Penmatsa, A., Wang, K. H., and Gouaux, E. (2013) X-ray structure of dopamine transporter elucidates antidepressant mechanism, *Nature 503*, 85-90.
39. Rawling, T., Cui, P.H. Duke, C.C. and Murray, M. (2010) Stereoselective synthesis of (Z)-15-octadecenoic acid and (Z)-16- nonadecenoic acid: Monounsaturated omega-3 fatty acids. *Lipids* 45, 159-165
40. Cui, P.H., Rawling, T., Bourget, K., Kim, T., Duke, C.C., Doddareddy, M.R., Hibbs, D.E., Zhou, F., Tattam, N.N., Petrovic, N. Murray, M. (2012) Antiproliferative and antimigratory actions of synthetic long chain n-3 monounsaturated fatty acids in breast cancer cells that overexpress cyclooxygenase-2. J Med Chem 55, 7163-7172.
41. Vandenberg, R. J., Mitrovic, A. D., and Johnston, G. A. (1998) Molecular basis for differential inhibition of glutamate transporter subtypes by zinc ions, *Mol Pharmacol 54*, 189-196.